もので，期待が大きい．

B. 癌進展制御におけるPTENの役割

過去十数年の研究で，広範囲にわたる*PTEN*遺伝子変異が同定され，また多くの癌腫がPTENの発現低下ないし機能不全によって発症することが明らかになった．様々な生物学的過程におけるPTENの役割についての解析は，いかにしてPTENの機能不全が癌のinitiationとprogressionに関与するかを明らかにしつつある．

1. 細胞運動性と極性

PTENとPIP_3は様々な種や細胞において細胞極性に関与する．PI3Kは下流のRHO，RAC1，CDC42活性化を介して，細胞膜ラフリングや細胞運動性，細胞伸展を亢進させる．一方，PTENは細胞遊走をフォスファターゼ活性非依存性に抑制する[12]．PTENは上皮において頂端面の細胞膜に局在し，PIP_3をPIP_2に転換する．PIP_2はannexin 2とCDC42を頂端面の細胞膜に動員してPAR6-aPKC複合体を形成することで細胞極性の形成と維持に働く[28]．したがって，PTEN-PI3K経路の制御不全は上皮細胞特性の喪失と間葉系細胞の特性の獲得，細胞運動性と浸潤性の亢進からなる上皮間葉転換（epithelial mesenchymal transition: EMT）の誘導につながる．

2. 癌微小環境

癌組織には，癌細胞の他に線維芽細胞や炎症細胞，血管内皮細胞などから構成される癌微小環境があり，癌細胞と間葉系細胞の相互作用は癌細胞の増殖と浸潤に重要である．線維芽細胞は癌微小環境を構築する主要成分の一つで，成長因子や血管新生因子，ケモカイン，細胞外マトリックスとそのturnover制御因子を産生し，癌細胞の増殖と浸潤を促進する．乳癌組織中の線維芽細胞においてPTENを欠損させると発癌性セクレトームが活性化され癌進展が亢進する[27,29]．また最近，癌微小環境から産生されるTGF-βによって肺癌細胞内のPTENがC2領域でリン酸化され，PTEN “Opened” 構造から “Closed” 構造への立体構造変化が起こり，フォスファターゼ活性が阻害されること，それに引き続いて肺癌細胞の細胞運動性とEMTと腫瘍形成能が亢進することが報告されている[30]．

3. 細胞老化

細胞老化とは，癌遺伝子の活性化や癌抑制遺伝子の損失・減少に伴って，細胞が不可逆性に増殖を停止することであり，細胞が癌化することを抑制する重要な防御機構である．PTENの発現減少は細胞増殖を亢進させる一方，PTENの完全欠損はmTORC1活性化を介するp53の発現亢進と，ETS2-$p16^{INK4a}$経路活性化を介するPTEN欠損誘導性細胞老化（PTEN loss-induced cellular senescence: PICS）とそれに引き続く腫瘍進展遅延を招く[23,24]．これらの事象は臨床的に，なぜ癌組織においてPTENの完全欠損があまりみられないか，なぜ進行期の癌組織ではPTENとp53が同時に発現低下していることが多くみられるのかを説明している．

4. 癌幹細胞

癌幹細胞とは，他の癌細胞と比較して抗癌剤や放射線療法に耐性であり，高率な腫瘍形成能をもつ少数の癌細胞群である．雑草の根のように癌治療中にも生き延び，癌再発の根幹となっている．正常幹細胞と同様に癌幹細胞も多分化能と自己複製能を有するが，正常幹細胞と癌幹細胞では自己複製能経路の遺伝子に変化があり，その相違を標的とした治療法の開拓は現在癌治療において最も注目されている分野の一つである．Zhangら[31]とYilmazら[32]は，正常造血幹細胞と白血病幹細

胞におけるPTENの役割について，PTEN欠損により正常造血幹細胞が枯渇し，白血病開始細胞(leukemia-initiating cells: LICs) の産生とそれに引き続く白血病発症が起こることを報告した．mTOR阻害剤であるrapamycin投与により，造血幹細胞における自己複製能の正常化とLICs産生抑制が生じることから，mTOR活性はPTEN欠損に伴う正常造血幹細胞枯渇とLICs産生の主要メディエーターであるといえる．この所見は，PTEN欠損とmTOR経路の過剰活性化により，p53，$p16^{INK4A}$，$p19^{ARF}$などのチェックポイント安全装置が活性化され，細胞老化とアポトーシスにより正常幹細胞と癌幹細胞が枯渇する報告[33]と一致する．以上のことより，正常幹細胞と癌幹細胞の差異におけるPTENの役割から，PTEN-mTOR経路は正常幹細胞を損なうことなく癌幹細胞を枯渇させることができる治療標的となり得ることが示唆される．

C．PTEN制御機構

PTENの発現レベルや機能，細胞内局在は，遺伝子変異による発現低下の他に，エピジェネティクス発現抑制，転写因子による制御，miRNAや競合内因性RNA（competitive endogenous RNA: ceRNA）による制御，翻訳後修飾，PTEN相互作用蛋白など，多岐にわたるメカニズムにより正にあるいは負に制御されている．

1．エピジェネティクス発現抑制，転写制御

正常組織ではPTENは恒常的に発現しているが，エピジェネティックな発現抑制，転写制御により発現レベルが劇的に変化する．多くの癌腫でプロモーター領域のメチル化によるPTENの発現抑制がみられる[34]．また多くの転写因子がPTENの発現を制御する．SNAIL，NF-κB，MYC，BMI-1，c-JUN，ID1，SALL4はPTENの発現を抑制し，p53，PPARγ，EGR1，CBF1はPTENの発現を促進する[3,20]．NOTCH1はMYCの発現を亢進し，CBF1の発現を抑制することで間接的にPTEN発現を抑制する．

2．non-coding RNAによる転写後制御機構

miRNAは20～25塩基からなるnon-coding RNAで，標的遺伝子のmRNAに結合し転写後翻訳調節の役割を担う．最近，多くのmiRNAがPTENの発現を抑制し，腫瘍伸展を亢進させることが報告されている．リンパ増殖性疾患においてmiR-17～92クラスターが，白血病とCowden病においてmiR-19が，また多くの癌腫においてmiR-21がPTEN発現を抑制する[3]．癌遺伝子MYCはmiR-19の発現亢進を介してPTEN発現を抑制する[35]．また最近Mouwらは，乳癌組織での細胞外マトリックス硬化はβカテニン核内移行とMYC発現を介してmiR-18a発現を亢進させ，標的分子であるPTENの発現低下と，手術症例の再発期間の短縮を来すことを報告している[36]．一方，PTENには自身のmRNAと比べてmiRNA標的配列を含めて塩基配列が高度に保存されている偽遺伝子，PTENP1が存在する．PTENP1はPTENのmRNAを標的とするmiRNAに対してデコイとして働きPTEN発現を上方制御するという興味深い報告がなされている[37]．

3．翻訳後修飾

いったん発現したPTEN蛋白は，リン酸化，アセチル化，酸化，ユビキチン化などにより様々な機能修飾を受ける．GSK3βとCK2はPTEN蛋白のC末tail領域をリン酸化し，PTENのフォスファターゼ活性を阻害するとともに細胞膜への局在を減少させる[3]．ROCKはPTEN C2領域をリン酸化し，フォスファターゼ活性を亢進，細胞膜への局在を増加させる[38]．RAKはPTENをリン酸化し，PTEN蛋白を安定化させる[39]．RAK欠損

によりPTENとE3ユビキチンリガーゼであるNEDD4-1との結合が増強し，PTENのポリユビキチン化とそれに引き続くPTENの分解が亢進する[40]．また前述したように，NEDD4-1によるLys13とLys289でのモノユビキチン化は，PTENの核内移行とそれに引き続くゲノム安定化に重要である[18]．

D．肺癌とPTEN

PHTSにおける肺癌の発症は稀であり，また小細胞肺癌および非小細胞肺癌組織における*PTEN*遺伝子変異の頻度はそれぞれ10%（1例/10例）および6%（3例/47例）と少ない[41,42]．一方，早期の非小細胞肺癌組織の24%において，プロモーター領域のメチル化によりPTEN発現が低下しており[43]，早期肺癌手術症例の予後不良因子とされている[44]．また，肺癌の74%の症例で癌組織中のPTEN蛋白発現が低下しており，肺腺癌組織におけるPTEN発現低下とAKT活性化は患者予後に相関する[45,46]．さらに，非小細胞肺癌症例の74%の症例でmiR-21発現亢進とそれに引き続くPTEN mRNAの発現減少がみられる[47]．PTENと治療感受性との関連について，EGFR-TKIの耐性要因として，*PTEN*遺伝子のホモ欠損や[48]，EGR1（PTEN発現を促進する転写因子）の核内移行阻害に伴うPTEN発現低下[49]が報告されている．

我々は細気管支肺胞上皮特異的にdoxycycline誘導性にPtenを欠損するマウスを作製し[50]，40～70週齢においてほぼ全例に肺腺癌を自然発症することを報告した．Pten欠損マウスでは，肺腺癌発症前の肺組織において細気管支肺胞上皮幹細胞（bronchioalveolar stem cells: BASCs）の数が増加していた．肺腺癌の起源はBASCsであるとされることから[51]，Pten欠損によるBASCsの増加が肺腺癌発症の一因である可能性が考えられた．さらにPten欠損マウスに生じた肺腺癌で高頻度にK-rasの変異がみられた．Pten欠損によるBASCsの増加によりK-rasなどの他の癌関連遺伝子の変異が起こりやすくなり，さらなるBASCsの増加が起こり肺腺癌を発症した可能性が考えられた．また，細気管支上皮特異的Pten欠損マウスでは，K-ras過剰発現による腺癌形成が加速していた[52]．

他の組織型とPTENとの関連について，Cuiらはp53/Rb二重欠損小細胞肺癌モデルマウスにおいてPtenをヘテロ欠損させると，小細胞肺癌の増大と転移が加速することを報告している[53]．またXuらは，LKB-1とPTENの二重欠損マウスが高率に肺扁平上皮癌を発症すること，LKB-1/PTEN二重欠損肺扁平上皮癌組織中に，三次移植まで扁平上皮癌形成能を有する細胞群（tumor-propagating cells)が存在することを報告した[54]．以上の所見から，PTEN発現低下は肺癌の発症と進展に密接に関わっていることが示唆され，PTEN-PI3K-AKT-mTOR経路は重要な肺癌治療標的であると考えられる．T790M変異によるEGFR-TKI耐性症例での肺腺癌組織中ではmTORが活性化していること，EGFR L858R＋T790M変異肺腺癌モデルにおいて，EGFR-TKI治療後にmTOR阻害剤を投与すること無増悪生存期間と全生存期間が延長することが報告されている[55]．現在，進行非小細胞肺癌に対する新規mTOR阻害剤の第Ⅰ相臨床試験が行われている[56]．

E．急性呼吸促迫症候群，肺線維症とPTEN

肺胞上皮細胞（alveolar epithelial cells: AECs）の損傷とそれに引き続く修復異常は，特発性肺線維症（IPF）や急性呼吸促迫症候群（ARDS）の病態進展に重要である[57,58]．正常肺では，AECsはタイトジャンクション（TJs）を介して互いに

密に接合した強固なバリアとして存在し，基底膜上に存在する．AECsの損傷が広範であったり，基底膜が断裂したりすると，正常な修復が起こらず，肺構築破壊を伴う線維化に陥る．これまでにAECs特異的integrin-α3欠損マウスで肺損傷後線維化が軽減した報告がある[59]．しかし，AECsバリア統合性の制御機構や内因性制御分子については明らかにされていなかった．

1．AECsバリア統合性保持と上皮PTEN

肺線維症について，これまでに線維芽細胞でのPTENの機能解析の報告はあるが[60,61]，上皮細胞PTENの臓器線維化における役割についての報告はない．我々は，後天的かつAECs特異的にPtenを欠損させたマウスを用いてARDS/肺線維症モデルを作成し，上皮PTENの役割を解析した[62]．AECs特異的Pten欠損マウスは野生型マウスと比較して肺損傷後に広範な肺水腫と線維化をきたし，低酸素血症により早期に死亡した．Pten欠損マウスでは肺損傷後の肺組織においてAEC細胞間の解離がみられ，TJs構成蛋白の発現低下と基底膜断裂の亢進がみられた．以上の結果から，肺上皮PTENは上皮バリア統合性保持を介してARDSと肺線維化の進展抑制に必須であることが示唆された（図4）．

2．AECsバリア統合性修復と上皮PTEN

我々は，修復期での上皮PTENの機能を解析するために，肺損傷後にAECs特異的にPtenを欠損させたマウスを作成した[62]．その結果，肺損傷早期相での肺水腫の程度は野生型とPten欠損マウスとでは差がなかった一方，修復期においてPten欠損マウスでは急性肺水腫の遷延と線維化の増悪がみられた．以上の結果から，急性期のみならず修復期におけるAECsでのPTEN発現も肺線維症の進展制御に重要と考えられた．この修復異常を反映して，Pten欠損マウスでは肺損傷後にAECs由来筋線維芽細胞数が増加していた．これらの表現形の責任分子として，AECs特異的Pten欠損マウスから単離したAECsにおいて，

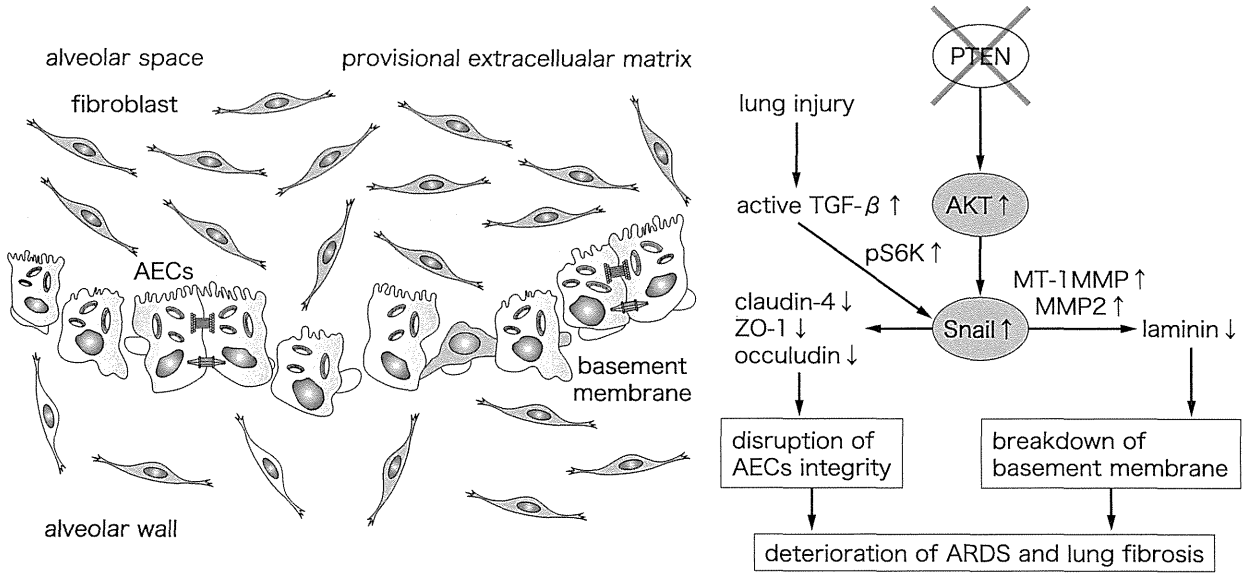

図4　上皮統合性維持によるPTENのARDSと肺線維症の進展制御

上皮PTEN欠損により，肺損傷後のtight junction破綻亢進が起こり，provisional extracellular matrixの肺胞腔内への滲出が増加し，fibroblastの肺胞腔内遊走・活性化亢進が生じる．また上皮PTEN欠損に伴い，肺損傷後の基底膜破綻亢進が起こり，上皮再生・遊走のための足場が喪失し，AECsバリア統合性再構築不全・修復不全に陥る．

AktとP70S6Kの活性化，SnailとMMP2とMT1-MMPの発現亢進がみられた．また，肺損傷後のPten欠損マウスにAKT阻害剤を腹腔内投与した結果，ARDSと肺線維化が軽減した．さらに，IPF患者肺組織のAECsにおいてPTEN発現低下とAKT活性化がみられた．興味深いことに，IPF患者組織ではPTENを標的とするmiR-21が過剰に発現していることが報告されており[63]，miRNA発現を介するPTEN発現低下によるエピジェネティクス分子機構により，上皮統合性が制御されていることが示唆される[64]．

F．その他の呼吸器疾患とPTEN

Kwakらは気管支喘息モデルにおいて，細気管支上皮でPTENを過剰発現させると，気道炎症と気道過敏性が軽減することを報告した[65]．呼吸器感染症へのPTENの関与について，骨髄球系特異的PTEN欠損マウスを用いた解析などにより，好中球におけるPTEN発現が殺菌能，走化性，血管外遊走と炎症部位への集積ならびに肺胞マクロファージの貪食能を負に制御することが報告されている[66-68]．

むすび

本稿では，呼吸器疾患におけるPTENの役割について，signaling pathwayや制御機構を含めて最近の知見をもとに概説した．PTENは癌発症と進展抑制に中心的な役割を果たすとともに，急性呼吸促迫症候群や肺線維症などの非腫瘍性疾患でも決定的なgatekeeperとして機能している．PTENに関する論文は最近急速に増加しており，現在9000編以上に及ぶ．細胞質と核内，細胞外を仕事場とする守備範囲の広さとPTEN固有のfunctional diversityから，今後も呼吸器疾患におけるPTENの新たな知見が次々と発見されていくと考えられる．細胞特異的な疾患治療開発を含めて，今後さらに基礎および臨床の両面から核心に迫る研究の展開に期待したい．

文献

1) Li J, Yen C, Liaw D, et al. PTEN, a putative protein tyrosine phosphatase gene mutated in human brain, breast, and prostate cancer. Science. 1997; 285: 1943-7.
2) Steck PA, Pershouse MA, Jasser SA, et al. Identification of a candidate tumour suppressor gene, MMAC1, at chromosome 10q23.3 that is mutated in multiple advanced cancers. Nat Genet. 1997; 15: 356-62.
3) Song MS, Salmena L, Pandolfi PP. The functions and regulation of the PTEN tumour suppressor. Nat Rev Mol Cell Biol. 2012; 13: 283-96.
4) Yin Y, Shen WH. PTEN: a new guardian of the genome. Oncogene. 2008; 27: 5443-53.
5) Suzuki A, de la Pompa JL, Stambolic V, et al. High cancer susceptibility and embryonic lethality associated with mutation of the PTEN tumor suppressor gene in mice. Curr Biol. 1998; 8: 1169-78.
6) Di Cristofano A, Pesce B, Cordon-Cardo C, et al. Pten is essential for embryonic development and tumour suppression. Nat Genet. 1998; 19: 348-55.
7) Eng C. PTEN: one gene, many syndromes. Hum Mutat. 2003; 22: 183-98.
8) Wu X, Hepner K, Castelino-Prabhu S, et al. Evidence for regulation of the PTEN tumor suppressor by a membrane-localized multi-PDZ domain containing scaffold protein MAGI-2. Proc Natl Acad Sci U S A. 2000; 97: 4233-8.
9) Valiente M, Andrés-Pons A, Gomar B, et al. Binding of PTEN to specific PDZ domains contributes to PTEN protein stability and phosphorylation by microtubule-associated serine/threonine kinases. J Biol Chem. 2005; 280: 28936-43.
10) Manning BD, Cantley LC. AKT/PKB signaling: navigating downstream. Cell. 2007; 129: 1261-74.
11) Maehama T, Dixon JE. The tumor suppressor, PTEN/MMAC1, dephosphorylates the lipid second messenger, phosphatidylinositol 3,4,5-trisphosphate. J Biol Chem. 1998; 273: 13375-8.

12) Tamura M, Gu J, Matsumoto K, et al. Inhibition of cell migration, spreading, and focal adhesions by tumor suppressor PTEN. Science. 1998; 280: 1614-7.
13) Gu J, Tamura M, Yamada KM. Tumor suppressor PTEN inhibits integrin- and growth factor-mediated mitogen-activated protein (MAP) kinase signaling pathways. J Cell Biol. 1998; 143: 1375-83.
14) Puc J, Keniry M, Li HS, et al. Lack of PTEN sequesters CHK1 and initiates genetic instability. Cancer Cell. 2005; 7: 193-204.
15) Shen WH, Balajee AS, Wang J, et al. Essential role for nuclear PTEN in maintaining chromosomal integrity. Cell. 2007; 128: 157-70.
16) Emerling BM, Weinberg F, Liu JL, et al. PTEN regulates p300-dependent hypoxia-inducible factor 1 transcriptional activity through Forkhead transcription factor 3a (FOXO3a). Proc Natl Acad Sci U S A. 2008; 105: 2622-7.
17) Song MS, Carracedo A, Salmena L, et al. Nuclear PTEN regulates the APC-CDH1 tumor-suppressive complex in a phosphatase-independent manner. Cell. 2011; 144: 187-99.
18) Trotman LC, Wang X, Alimonti A, et al. Ubiquitination regulates PTEN nuclear import and tumor suppression. Cell. 2007; 128: 141-56.
19) Vogelstein B, Lane D, Levine AJ. Surfing the p53 network. Nature. 2000; 408: 307-10.
20) Stambolic V, MacPherson D, Sas D, et al. Regulation of PTEN transcription by p53. Mol Cell. 2001; 8: 317-25.
21) Li AG, Piluso LG, Cai X, et al. Mechanistic insights into maintenance of high p53 acetylation by PTEN. Mol Cell. 2006; 23: 575-87.
22) Lian Z, Di Cristofano A. Class reunion: PTEN joins the nuclear crew. Oncogene. 2005; 24: 7394-400.
23) Salmena L, Carracedo A, Pandolfi PP. Tenets of PTEN tumor suppression. Cell. 2008; 133: 403-14.
24) Chen Z, Trotman LC, Shaffer D, et al. Crucial role of p53-dependent cellular senescence in suppression of Pten-deficient tumorigenesis. Nature. 2005; 436: 725-30.
25) Putz U, Howitt J, Doan A, et al. The tumor suppressor PTEN is exported in exosomes and has phosphatase activity in recipient cells. Sci Signal. 2012; 5: ra70.
26) Hopkins BD, Fine B, Steinbach N, et al. A secreted PTEN phosphatase that enters cells to alter signaling and survival. Science. 2013; 341: 399-402.
27) Trimboli AJ, Cantemir-Stone CZ, Li F, et al. Pten in stromal fibroblasts suppresses mammary epithelial tumours. Nature. 2009; 461: 1084-91.
28) Martin-Belmonte F, Gassama A, Datta A, et al. PTEN-mediated apical segregation of phosphoinositides controls epithelial morphogenesis through Cdc42. Cell. 2007; 128: 383-97.
29) Bronisz A, Godlewski J, Wallace JA, et al. Reprogramming of the tumour microenvironment by stromal PTEN-regulated miR-320. Nat Cell Biol. 2011; 14: 159-67.
30) Aoyama D, Hashimoto N, Sakamoto K, et al. Involvement of TGFβ-induced phosphorylation of the PTEN C-terminus on TGFβ-induced acquisition of malignant phenotypes in lung cancer cells. PLoS One. 2013; 8: e81133.
31) Zhang J, Grindley JC, Yin T, et al. PTEN maintains haematopoietic stem cells and acts in lineage choice and leukaemia prevention. Nature. 2006; 441: 518-22.
32) Yilmaz OH, Valdez R, Theisen BK, et al. Pten dependence distinguishes haematopoietic stem cells from leukaemia-initiating cells. Nature. 2006; 441: 475-82.
33) Lee JY, Nakada D, Yilmaz OH, et al. mTOR activation induces tumor suppressors that inhibit leukemogenesis and deplete hematopoietic stem cells after Pten deletion. Cell Stem Cell. 2010; 7: 593-605.
34) Hollander MC, Blumenthal GM, Dennis PA. PTEN loss in the continuum of common cancers, rare syndromes and mouse models. Nat Rev Cancer. 2011; 11: 289-301.
35) Mu P, Han YC, Betel D, et al. Genetic dissection of the miR-17~92 cluster of microRNAs in Myc-induced B-cell lymphomas. Genes Dev. 2009; 23: 2806-11.
36) Mouw JK, Yui Y, Damiano L, et al. Tissue mechanics modulate microRNA-dependent PTEN expression to regulate malignant progression. Nat Med. 2014; 20: 360-7.
37) Poliseno L, Salmena L, Zhang J, et al. A coding-

independent function of gene and pseudogene mRNAs regulates tumour biology. Nature. 2010; 465: 1033-8.
38) Li Z, Dong X, Wang Z, et al. Regulation of PTEN by Rho small GTPases. Nat Cell Biol. 2005; 7: 399-404.
39) Yim EK, Peng G, Dai H, et al. Rak functions as a tumor suppressor by regulating PTEN protein stability and function. Cancer Cell. 2009; 15: 304-14.
40) Wang X, Trotman LC, Koppie T, et al. NEDD4-1 is a proto-oncogenic ubiquitin ligase for PTEN. Cell. 2007; 128: 129-39.
41) Yokomizo A, Tindall DJ, Drabkin H, et al. PTEN/MMAC1 mutations identified in small cell, but not in non-small cell lung cancers. Oncogene. 1998; 17: 475-9.
42) Kohno T, Takahashi M, Manda R, et al. Inactivation of the PTEN/MMAC1/TEP1 gene in human lung cancers. Genes Chromosomes Cancer. 1998; 22: 152-6.
43) Soria JC, Lee HY, Lee JI, et al. Lack of PTEN expression in non-small cell lung cancer could be related to promoter methylation. Clin Cancer Res. 2002; 8: 1178-84.
44) Buckingham L, Penfield Faber L, Kim A, et al. PTEN, RASSF1 and DAPK site-specific hypermethylation and outcome in surgically treated stage I and II nonsmall cell lung cancer patients. Int J Cancer. 2010; 126: 1630-9.
45) Marsit CJ, Zheng S, Aldape K, et al. PTEN expression in non-small-cell lung cancer: evaluating its relation to tumor characteristics, allelic loss, and epigenetic alteration. Hum Pathol. 2005; 36: 768-76.
46) Tang JM, He QY, Guo RX, et al. Phosphorylated Akt overexpression and loss of PTEN expression in non-small cell lung cancer confers poor prognosis. Lung Cancer. 2006; 51: 181-91.
47) Zhang JG, Wang JJ, Zhao F, et al. MicroRNA-21 (miR-21) represses tumor suppressor PTEN and promotes growth and invasion in non-small cell lung cancer (NSCLC). Clin Chim Acta. 2010; 411: 846-52.
48) Sos ML, Koker M, Weir BA, et al. PTEN loss contributes to erlotinib resistance in EGFR-mutant lung cancer by activation of Akt and EGFR. Cancer Res. 2009; 69: 3256-61.
49) Yamamoto C, Basaki Y, Kawahara A, et al. Loss of PTEN expression by blocking nuclear translocation of EGR1 in gefitinib-resistant lung cancer cells harboring epidermal growth factor receptor-activating mutations. Cancer Res. 2010; 70: 8715-25.
50) Yanagi S, Kishimoto H, Kawahara K, et al. Pten controls lung morphogenesis, bronchioalveolar stem cells, and onset of lung adenocarcinomas in mice. J Clin Invest. 2007; 117: 2929-40.
51) Kim CF, Jackson EL, Woolfenden AE, et al. Identification of bronchioalveolar stem cells in normal lung and lung cancer. Cell. 2005; 121: 823-35.
52) Iwanaga K, Yang Y, Raso MG, et al. Pten inactivation accelerates oncogenic K-ras-initiated tumorigenesis in a mouse model of lung cancer. Cancer Res. 2008; 68: 1119-27.
53) Cui M, Augert A, Rongione M, et al. PTEN is a potent suppressor of small cell lung cancer. Mol Cancer Res. 2014; 12: 654-9.
54) Xu C, Fillmore CM, Koyama S, et al. Loss of Lkb1 and Pten leads to lung squamous cell carcinoma with elevated PD-L1 expression. Cancer Cell. 2014; 25: 590-604.
55) Kawabata S, Mercado-Matos JR, Hollander MC, et al. Rapamycin prevents the development and progression of mutant epidermal growth factor receptor lung tumors with the acquired resistance mutation T790M. Cell Rep. 2014; 7: 1824-32.
56) Mita MM, Mita AC, Chu QS, et al. Phase I trial of the novel mammalian target of rapamycin inhibitor deforolimus (AP23573; MK-8669) administered intravenously daily for 5 days every 2 weeks to patients with advanced malignancies. J Clin Oncol. 2008; 26: 361-7.
57) King TE Jr, Pardo A, Selman M. Idiopathic pulmonary fibrosis. Lancet. 2011; 378: 1949-61.
58) Chapman HA. Epithelial-mesenchymal interactions in pulmonary fibrosis. Annu Rev Physiol. 2011; 73: 413-35.
59) Kim KK, Wei Y, Szekeres C, et al. Epithelial cell alpha3beta1 integrin links beta-catenin and Smad signaling to promote myofibroblast formation and pulmonary fibrosis. J Clin Invest. 2009; 119:

213-24.
60) Xia H, Diebold D, Nho R, et al. Pathological integrin signaling enhances proliferation of primary lung fibroblasts from patients with idiopathic pulmonary fibrosis. J Exp Med. 2008; 205: 1659-72.
61) White ES, Atrasz RG, Hu B, et al. Negative regulation of myofibroblast differentiation by PTEN (Phosphatase and Tensin Homolog Deleted on chromosome 10). Am J Respir Crit Care Med. 2006; 173: 112-21.
62) Miyoshi K, Yanagi S, Kawahara K, et al. Epithelial Pten controls acute lung injury and fibrosis by regulating alveolar epithelial cell integrity. Am J Respir Crit Care Med. 2013; 187: 262-75.
63) Liu G, Friggeri A, Yang Y, et al. miR-21 mediates fibrogenic activation of pulmonary fibroblasts and lung fibrosis. J Exp Med. 2010; 207: 1589-97.
64) Selman M, Pardo A. Revealing the pathogenic and aging-related mechanisms of the enigmatic idiopathic pulmonary fibrosis. an integral model. Am J Respir Crit Care Med. 2014; 189: 1161-72.
65) Kwak YG, Song CH, Yi HK, et al. Involvement of PTEN in airway hyperresponsiveness and inflammation in bronchial asthma. J Clin Invest. 2003; 111: 1083-92.
66) Ittner A, Block H, Reichel CA, et al. Regulation of PTEN activity by p38δ-PKD1 signaling in neutrophils confers inflammatory responses in the lung. J Exp Med. 2012; 209: 2229-46.
67) Hubbard LL, Wilke CA, White ES, et al. PTEN limits alveolar macrophage function against *Pseudomonas aeruginosa* after bone marrow transplantation. Am J Respir Cell Mol Biol. 2011; 45: 1050-8.
68) Li Y, Jia Y, Pichavant M, et al. Targeted deletion of tumor suppressor PTEN augments neutrophil function and enhances host defense in neutropenia-associated pneumonia. Blood. 2009; 113: 4930-41.

© 2015. Published by The Company of Biologists Ltd | Journal of Cell Science (2015) 128, 1051–1063 doi:10.1242/jcs.163683

RESEARCH ARTICLE

Basolateral secretion of Wnt5a in polarized epithelial cells is required for apical lumen formation

Hideki Yamamoto[1], Chihiro Awada[2,*], Shinji Matsumoto[1], Tomoyuki Kaneiwa[1], Takayuki Sugimoto[1], Toshifumi Takao[2] and Akira Kikuchi[1,‡]

ABSTRACT

Wnt5a regulates planar cell polarity in epithelial cells, but it remains to be determined whether Wnt5a and its receptors are sorted apically or basolaterally, and how Wnt5a signaling is involved in apical and basolateral polarization. We found that Wnt5a was secreted basolaterally in polarized kidney epithelial cells. The basolateral secretion of Wnt5a required Wntless (Wls), clathrin and adaptor protein 1 (AP-1). Wnt5a receptors were also localized to the basolateral membranes, but their sorting did not require Wls. Wnt5a-induced signaling was stimulated more efficiently at the basolateral side than the apical side of epithelial cells. Knockdown of Wnt5a delayed apical lumen formation of the epithelial cyst, and these phenotypes were rescued by wild-type Wnt5a, but not by a Wnt5a mutant that is secreted apically. Although apoptosis was not required for apical lumen formation in a wild-type cyst, apoptosis was necessary for eliminating luminal cells in a Wnt5a-depleted cyst. These results suggest that Wnt5a and its receptors are sorted to their correct destination by different mechanisms and that the basolateral secretion of Wnt5a is necessary for apical lumen formation in the epithelial cyst.

KEY WORDS: Epithelial cells, Glycosylation, Polarity, Lumen, Wnt5a

INTRODUCTION

The generation and maintenance of epithelial cell polarity requires the correct delivery of newly synthesized and endocytosed proteins to apical or basolateral membrane domains (Yeaman et al., 1999). To establish apical-basolateral polarity, cells must sense their environment, which can be mediated by the interaction of cells with the extracellular matrix, including basement membrane proteins. Cells also recognize soluble factors, such as morphogens and growth factors, and activate signaling pathways to support the orientation of their polarity (Bryant and Mostov, 2008). As an example of a soluble factor, Wnt5a promotes the induction of single-cell polarization in rat intestinal epithelial cells (IEC6 cells) (Gon et al., 2013). Wnt5a is a member of the Wnt family, which is a large family of secreted molecules that play an important role in developmental processes; defective Wnt signaling in postnatal life causes disease in humans (Kikuchi et al., 2011; Logan and Nusse, 2004; Polakis, 2007). Our previous study showed that when IEC6 cells were seeded on thick Matrigel containing basement membrane proteins, a single cell was polarized cell autonomously, with an F-actin cap forming on the opposite side to Matrigel; knockdown of Wnt5a inhibited this phenotype (Gon et al., 2013). In cancer cells, Frizzled-2 (Fz2), a Wnt5a receptor, forms a complex with integrin α2, and Dvl, a cytoplasmic protein that mediates Wnt5a signaling, interacts with focal adhesion kinase (FAK), thereby enhancing cell-to-substrate adhesion (Matsumoto et al., 2010). Thus, Wnt5a and its receptors appear to sort to the basolateral membranes of polarized epithelial cells and might be required for the formation of apical-basolateral polarity.

Wnt proteins are post-translationally modified with oligosaccharides and lipids during their synthesis (Harterink and Korswagen, 2012; Komekado et al., 2007; Kurayoshi et al., 2007; Takada et al., 2006; Willert et al., 2003). Our previous study also revealed that the majority of Wnt3a and Wnt11 are secreted basolaterally and apically, respectively, in polarized Madin-Darby canine kidney (MDCK) epithelial cells (Yamamoto et al., 2013). The basolateral traffic of Wnt3a requires adaptor protein 1 (AP-1) and clathrin, which are known to be important for the sorting of basolateral membrane proteins (Boehm and Bonifacino, 2001; Deborde et al., 2008; Fölsch, 2005). It is generally thought that glycosylation of secretary proteins is necessary for their folding in the endoplasmic reticulum (ER) or exit from the ER (Spiro, 2002). Wnt3a and Wnt11 were glycosylated at multiple Asn residues, and their glycosylation profiles differed (Yamamoto et al., 2013). The complex-type glycan attached to Wnt11 at the N-terminal region is unique, and glycosylation is necessary for the apical secretion of Wnt11.

In addition, Wnt3a and Wnt11 are modified with palmitoleic acid at a conserved Ser residue (Takada et al., 2006; Yamamoto et al., 2013). The lipidation of Wnt3a and Wnt11 occurs in the ER, is catalyzed by porcupine and is essential for their exit from the ER. Wntless (Wls), which plays a crucial role in the trafficking of Wnt, recognizes palmitoleic-acid-modified Wnts in the ER and cycles between the plasma membranes and the ER through the Golgi (Port and Basler, 2010; Yu et al., 2014). Wls itself is trafficked to the basolateral membranes and its recycling is not required for the apical sorting of Wnt11 from the trans-Golgi (Yamamoto et al., 2013). Crystal structural analyses have revealed that the lipid modification of *Xenopus* Wnt8 inserts into the groove of the extracellular domain of mouse Fz8, suggesting the necessity of lipid modification of Wnts for the recognition and activation of receptors (Janda et al., 2012). Thus, post-translational modifications have important roles in the secretion and action of Wnts, and determination of Wnt5a modifications

[1]Department of Molecular Biology and Biochemistry, Graduate School of Medicine, Osaka University, 2-2 Yamadaoka, Suita, Osaka 565-0871, Japan. [2]Laboratory of Protein Profiling and Functional Proteomics, Institute for Protein Research, Osaka University, 3-2 Yamadaoka, Suita, Osaka 565-0871, Japan. *Present address: R&D Dept. Bio Medical Project, Pharma Foods International Co., Ltd., 1-49 Goryo-Ohara, Nishikyo-ku, Kyoto 615-8245, Japan.

‡Author for correspondence (akikuchi@molbiobc.med.osaka-u.ac.jp)

Received 21 September 2014; Accepted 17 December 2014

Journal of Cell Science

Journal of Cell Science (2015) 128, 1051–1063 doi:10.1242/jcs.163683

using mass spectrometry is necessary for the understanding of Wnt5a signaling.

Low-density lipoprotein receptor-related protein 6 (LRP6), receptor tyrosine kinase-like orphan receptor 2 (Ror2) and receptor-like tyrosine kinase (Ryk) function as co-receptors for Wnt3a, Wnt5a and Wnt11, respectively (Kim et al., 2008; Nishita et al., 2010; Yamamoto et al., 2006), although their cross-reactivity with other Wnts has also been reported (Lu et al., 2004; Yoshikawa et al., 2003). To transmit signals efficiently, these receptors need to be sorted to the same location as their specific Wnts. However, the mechanism underlying how they are sorted to their specific destinations is largely unknown. To elucidate the common and unique mechanisms in the polarized secretion of Wnt family members, we examined the polarized sorting of Wnt5a and its receptors. Here, we show the basolateral trafficking mechanisms of Wnt5a and its receptors. Furthermore, we examine the roles of Wnt5a polarized secretion in apical lumen formation of the epithelial cyst, and we demonstrate that basolaterally but not apically secreted Wnt5a promotes cell-to-substrate adhesion and activates Rac, thereby enhancing apical lumen formation without apoptosis.

RESULTS

Polarized secretion of Wnt5a

MDCK cells are commonly used in apical and basolateral polarization experiments with two-dimensional (2D) and 3D cultures. There are two types of MDCK cells: MDCK type I (MDCK I) and MDCK type II (MDCK II). The difference between the two types of MDCK cells is based on low (MDCK I) and high (MDCK II) passages of parent cell lines (Dukes et al., 2011). In addition, MDCK I cells have higher trans-epithelial electric resistance than MDCK II cells because they lack claudin-2 expression (Furuse et al., 2001). In MDCK I cells, *Wnt4*, *Wnt5a* and *Wnt7a* mRNAs were expressed at higher levels than *Wnt1*, *Wnt3*, *Wnt5b* and *Wnt11* mRNAs, whereas *Wnt5a* mRNA expression was lower than *Wnt4* and *Wnt7a* mRNA expression in MDCK II cells (supplementary material Fig. S1A). Western blot analysis revealed that endogenous Wnt5a was detected in MDCK I cells, but not in MDCK II cells (supplementary material Fig. S1B). When MDCK cells were cultured as a monolayer on a filter support (2D culture) (Gottardi et al., 1995), podocalyxin (an apical membrane marker) and transferrin receptor (TfR, a basolateral membrane receptor) were clearly sorted to apical and basolateral membranes, respectively (Fig. 1A). Under these conditions, the majority of endogenous Wnt5a in MDCK I cells was secreted basolaterally (Fig. 1A). To show the trafficking of Wnt5a more clearly, Wnt5a was stably expressed in MDCK I and MDCK II cells (MDCK I/Wnt5a and MDCK II/Wnt5a; supplementary material Fig. S1C). Exogenously expressed Wnt5a was secreted basolaterally in both cell lines (Fig. 1B).

These findings were confirmed using MDCK II cysts in 3D Matrigel culture. When Wnt5a was transiently expressed in MDCK II cells and the cells were permeabilized, Wnt5a was detected in the cytoplasm but not in the apical lumens, whereas when the cells were stained without permeabilization, Wnt5a was detected on the basal membranes (Fig. 1C). In MDCK II/Wnt5a cells with permeabilization, Wnt5a was observed in the immediate vicinity of basal membranes but not in the apical lumen (Fig. 1C). In subsequent experiments, we overexpressed Wnt5a and Wnt receptors in MDCK II cells to examine its trafficking mechanisms, and knocked down endogenous Wnt5a in MDCK I cells to examine its function.

Wls is essential for the secretion of Wnts, and is trafficked to the basolateral membranes by AP-1 and clathrin from the trans-Golgi network (Port and Basler, 2010; Yamamoto et al., 2013). Consistent with these observations, knockdown of Wls completely suppressed Wnt5a secretion in polarized MDCK II/Wnt5a cells, although the polarized distribution of podocalyxin and TfR was not impaired (Fig. 1D; supplementary material Fig. S1D). Clathrin and AP-1A, AP-1B and AP-4 sort cargo proteins to the basolateral membranes in epithelial cells (Boehm and Bonifacino, 2001; Deborde et al., 2008; Fölsch, 2005; Gravotta et al., 2012; Simmen et al., 2002). Knockdown of clathrin or μ1A and μ1B (also known as AP1M1 and AP1M2, respectively), which are medium subunits of AP-1A and AP-1B, respectively, disturbed the polarized sorting of TfR but not that of podocalyxin (Fig. 1E; supplementary material Fig. S1D,E). Under these conditions, the basolateral secretion of Wnt5a was severely suppressed (Fig. 1E). However, the depletion of μ4 (also known as AP4M1; a medium subunit of AP-4) did not affect the polarized distribution of Wnt5a, podocalyxin and TfR (Fig. 1F; supplementary material Fig. S1D). μ1B–HA expression rescued the phenotypes observed in μ1A- and μ1B-depeleted cells (Fig. 1G), excluding small interfering (si)RNA off-target effects. These results suggest that Wls, clathrin and AP-1 are important for the sorting of Wnt5a to the basolateral membrane.

Post-translational modification of Wnt5a

Because post-translational modifications of secretory proteins are important for their trafficking, we determined the glycan profiles of Wnt5a. Wnt5a has four possible *N*-glycosylation sites; namely, Asn-X-Ser/Thr, including N114, N120, N312 and N326 (Kurayoshi et al., 2007). Tryptic peptides of purified Wnt5a were subjected to nano-flow liquid chromatography followed by matrix-associated laser desorption/ionization mass spectrometry (MALDI-MS). About 74.3% of the entire Wnt5a amino acid sequence was covered; N114, N312 and N326 were glycosylated with high-mannose, hybrid and high-mannose-type oligosaccharides, respectively, but N120 was not glycosylated (supplementary material Table S1). Further analyses of tryptic peptides using nano-flow liquid chromatography/electrospray ionization mass spectrometry (LC/ESI-MS) confirmed that glycans were attached to N114, N312 and N326 of Wnt5a (Fig. 2; supplementary material Table S2).

When all glycosylation sites were mutated, Wnt5a was never secreted (Kurayoshi et al., 2007). To investigate the role of each glycan of Wnt5a in secretion, various combinations of mutations were added to the Wnt5a glycosylation sites (supplementary material Fig. S2A). Wnt5aN114Q/N120Q (N120 is glycosylated when N114 is mutated), Wnt5aN312Q, Wnt5aN326Q or Wnt5aN312Q/N326Q showed similar secretion levels to wild-type Wnt5a. By contrast, Wnt5aN114Q/N120Q/N312Q or Wnt5aN114Q/N120Q/N326Q completely impaired secretion. These results show that glycosylation at N114 alone, but not glycosylation at N312 or N326 alone, is sufficient for Wnt5a secretion, thereby suggesting that glycosylation at N114 is important for maintaining the overall folded structure of Wnt5a.

A lipid-modified peptide was also observed among the peptides identified by MALDI-tandem mass spectrometry (MALDI-MS/MS) (supplementary material Table S1). The peptide containing S244, observed at m/z 1455.9 (supplementary material Fig. S2B), was identified as the peptide with the monounsaturated fatty acid (C16:1), palmitoleic acid. The site of lipidation was clearly

Journal of Cell Science (2015) 128, 1051–1063 doi:10.1242/jcs.163683

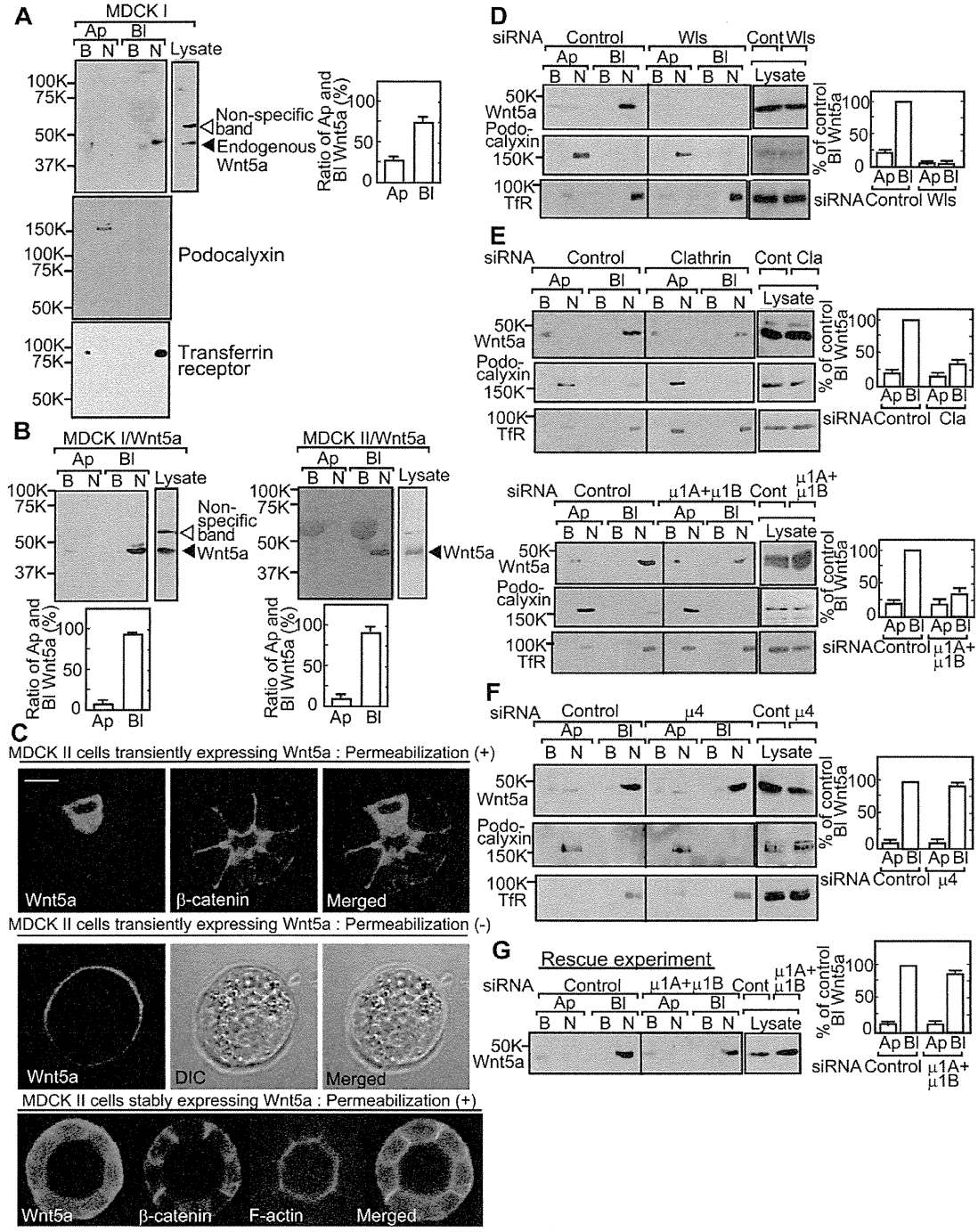

Fig. 1. See next page for legend.

identified as S244 by MALDI-MS/MS (supplementary material Fig. S2C), indicating that Wnt5a is modified with palmitoleic acid as are Wnt3a and Wnt11 (Takada et al., 2006; Yamamoto et al., 2013). In addition, Wnt5aS244A failed to be secreted (supplementary material Fig. S2D), confirming that the modification with palmitoleic acid is essential for Wnt secretion.

Addition of glycans to the N-terminal region of Wnt5a induces its apical secretion

We have previously shown that the complex-type glycan attached to N40 of Wnt11 is essential for its apical secretion, and that galectin-3, a galactose-binding lectin, is required for the apical secretion of Wnt11 (Yamamoto et al., 2013). Given that Wnt5a lacks a glycosylation site in the N-terminal region, Leu68 was

Journal of Cell Science (2015) 128, 1051–1063 doi:10.1242/jcs.163683

Fig. 1. Polarized secretion of Wnt5a. (A) MDCK I cells seeded on a Transwell polycarbonate filter were subjected to the apical-basolateral sorting assay. Soluble Wnt5a was detected in the precipitates using Blue–Sepharose from the apical media, and membrane-associated Wnt5a was observed in the precipitates using Neutravidin–agarose from the basolateral membranes. Wnt5a signals were quantified using NIH Imaging and the results were expressed as the ratio of Wnts between apical (Ap) and basolateral (Bl) fractions. Podocalyxin and transferrin receptor (TfR) were used as apical and basolateral membrane protein markers, respectively. Results are shown as means±s.e.m. from four independent experiments. B, precipitation using Blue–Sepharose; N, precipitation using Neutravidin–agarose. (B) MDCK I/Wnt5a and MDCK II/Wnt5a cells were subjected to the apical-basolateral sorting assay. (C) MDCK II cells transiently or stably expressing Wnt5a were cultured in 3D Matrigel, and the cysts with (+) or without (−) permeabilization were stained with the indicated antibodies or Alexa-Fluor-633-conjugated phalloidin to visualize F-actin, or observed by relief-contrast microscopy (DIC). F-actin and β-catenin were used as apical and basolateral markers, respectively. Scale bar: 10 μm. (D) MDCK II/Wnt5a cells were transfected with control (cont) or Wls siRNA, and the cells were then subjected to the apical-basolateral sorting assay. The Wnt5a signal was precipitated using Neutravidin–agarose in the control basolateral fraction, which was set to 100%. (E,F) MDCK II/Wnt5a cells were transfected with siRNAs for clathrin (Cla) (E), μ1A and μ1B (E) or μ4 (F), and the cells were subjected to the apical-basolateral sorting assay. (G) MDCK II/Wnt5a cells stably expressing μ1B–HA were transfected with siRNAs for μ1A and μ1B, and the cells were then subjected to the apical-basolateral sorting assay.

mutated to Asn to generate the amino acid sequence N68-X-S70, which is a possible glycosylation site (Fig. 3A). Wild-type Wnt5a secreted from MDCK II/Wnt5a cells showed different migration patterns by SDS-PAGE upon treatment with peptide: N-glycosidase F (PNGase F), which cleaves N-linked glycans, and upon treatment with endoglycosidase H_f (Endo H_f), which cleaves high-mannose and hybrid-type glycans, but not the complex-type glycan (Fig. 3B). This indicates that Wnt5a is heterogeneously glycosylated, which is consistent with the results of mass spectrometric analyses. Wnt5aL68N secreted from MDCK II/Wnt5aL68N cells (supplementary material Fig. S1G) exhibited lower mobility by SDS-PAGE than wild-type Wnt5a owing to the addition of glycan, and the amount of Endo H_f-resistant glycan increased (Fig. 3B), indicating that the complex type was attached to Wnt5aL68N. In contrast to wild-type Wnt5a, Wnt5aL68N was secreted apically in polarized MDCK II/Wnt5aL68N cells (Fig. 3B). Basally secreted Wnt5a was associated with membranes (see 'N' in Fig. 3B), whereas apically secreted Wnt5a was present in the medium (see 'B' in Fig. 3B), suggesting that Wnt5a might interact with the basement membranes. Wnt5aL68N in the conditioned medium induced a mobility shift of Dvl2 in NIH3T3 cells at a similar efficiency to that of control Wnt5a conditioned medium (Fig. 3C), suggesting that Wnt5aL68N is active.

Kifunensine and deoxymannojirimycin (dMM) inhibit ER-α-mannosidase I and Golgi-α-mannosidase I, respectively (Elbein et al., 1990; Fuhrmann et al., 1984). Gnt-I (also known as MGAT1), which is one of six *N*-acetylglucosamine transferases in vertebrates, initiates the formation of hybrid- and/or complex-type glycan (Rademacher et al., 1988). Treatment of MDCK II/Wnt5aL68N cells with kifunensine and dMM changed the

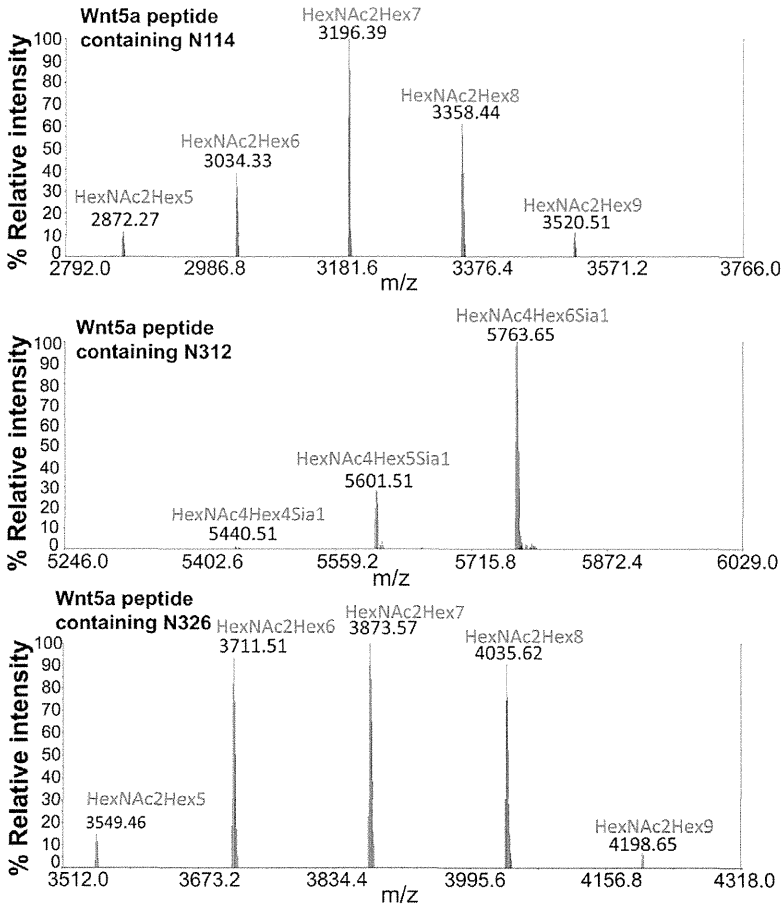

Fig. 2. Determination of the glycan profiles of Wnt5a. Wnt5a glycopeptides that eluted after 32.1 (N114), 36.5 (N312) and 28.6 min (N326) from nano-flow liquid chromatography were analyzed by ESI-MS. The mass spectra were deconvoluted to singly charged ions.

Journal of Cell Science (2015) 128, 1051–1063 doi:10.1242/jcs.163683

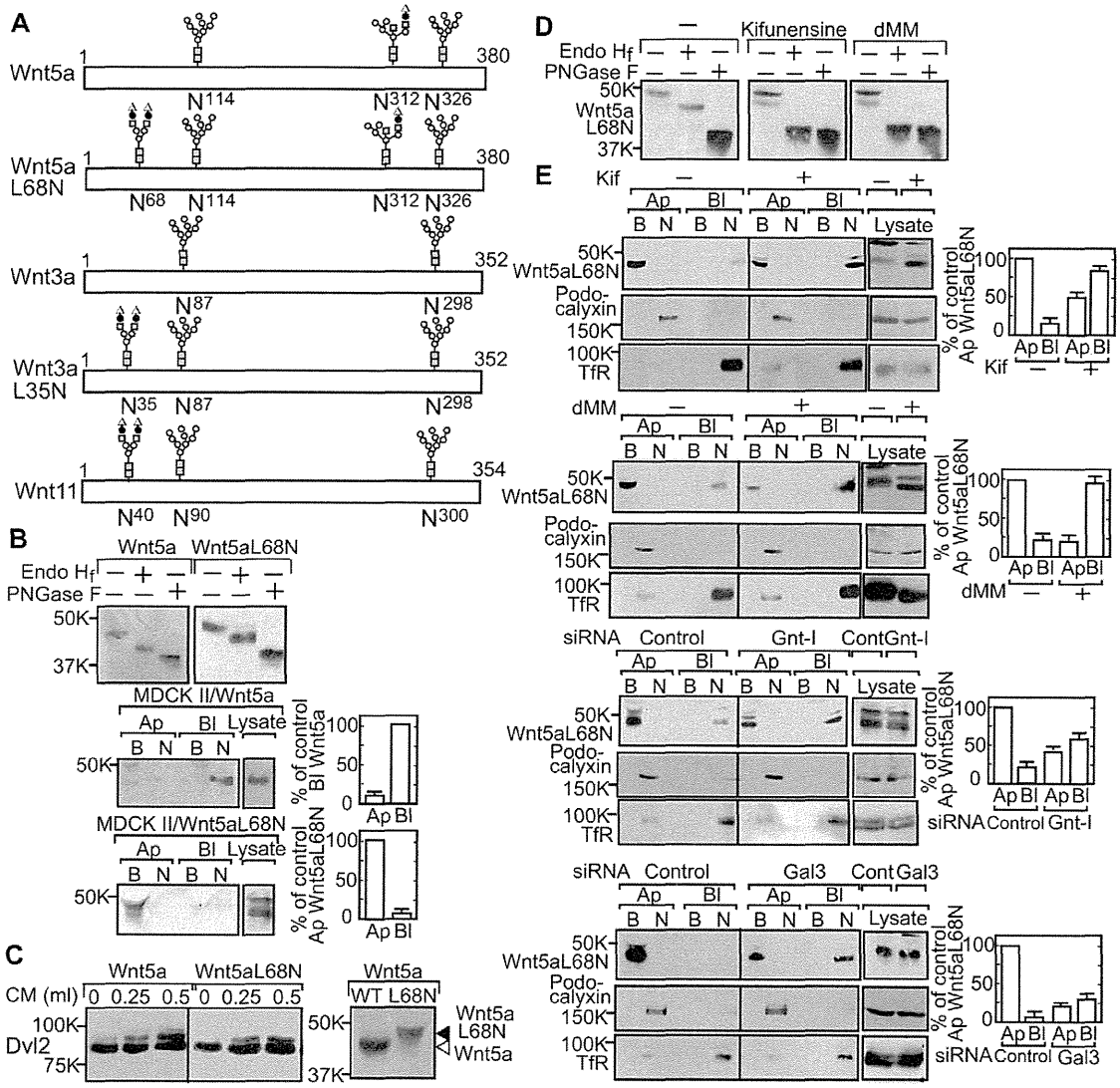

Fig. 3. Addition of glycans to the N-terminal region of Wnt5a induces its apical secretion. (A) Glycan profiles of Wnt5a, Wnt5aL68N, Wnt3a, Wnt3aL35N and Wnt11 are shown. (B) Wnt5a or Wnt5aL68N in conditioned medium from MDCK II cells was precipitated using Blue–Sepharose, and the precipitates were treated with Endo H_f or PNGase F, and then probed with anti-Wnt5a antibody (upper panels). MDCK II/Wnt5a or MDCK II/Wnt5aL68N cells were subjected to the apical-basolateral sorting assay (middle and lower panels). The signal of Wnt5a was precipitated using Neutravidin–agarose in the control basolateral (Bl) fraction and the signal of Wnt5aL68N was precipitated using Blue–Sepharose in the control apical (Ap) fraction was set to 100%. B, precipitation using Blue–Sepharose; N, precipitation using Neutravidin–agarose. (C) NIH3T3 cells were stimulated with the indicated amounts of Wnt5a- or Wnt5aL68N-containing conditioned medium (CM) from L cells for 2 h, and lysates were then probed with anti-Dvl2 antibody (left two panels). Conditioned media (20 µl) containing Wnt5a or Wnt5aL68N are shown in the right panel. (D) MDCK II/Wnt5aL68N cells were treated with kifunensine (kif) or deoxymannojirimycin (dMM), and Wnt5aL68N in conditioned medium was then precipitated using Blue–Sepharose. The precipitates were treated with Endo H_f or PNGase F and then probed with anti-Wnt5a antibody. (E) MDCK II/Wnt5aL68N cells were treated with kif or dMM, or transfected with Gnt-I or galectin 3 (Gal3) siRNA, and the cells were subjected to the apical-basolateral sorting assay. cont, control. Results are shown as means±s.e.m. from four independent experiments.

sensitivity of Wnt5aL68N to Endo H_f (Fig. 3D) and inhibited its apical secretion (Fig. 3E). siRNAs for Gnt-I and galectin-3 inhibited the apical secretion of Wnt5aL68N (Fig. 3E; supplementary material Fig. S1F). By contrast, these manipulations did not affect the polarized distribution of podocalyxin and TfR (Fig. 3E). Therefore, prevention of the maturation of the hybrid or complex-type glycan from the high-mannose-type glycan on Wnt5aL68N by these manipulations would impair its apical secretion.

Similar to Wnt5a, Leu35 was mutated to Asn in Wnt3a (Wnt3aL35N), and Wnt3aL35N was additionally modified with the complex-type glycan and secreted apically (Fig. 4A; supplementary material Fig. S1H). Treatment with kifunensine, dMM and siRNAs for Gnt-I and galectin-3 inhibited the apical secretion of Wnt3aL35N (Fig. 4B). Wnt3aL35N induced the accumulation of β-catenin to a similar degree as wild-type Wnt3a (Fig. 4C). These results suggest that the addition of complex-type glycan to the N-terminal region is sufficient for Wnt5a and Wnt3a to be secreted apically without losing their activities. Therefore, one amino acid substitution at the appropriate region of Wnts might be sufficient for Wnts to change their sorting destination.

Journal of Cell Science (2015) 128, 1051–1063 doi:10.1242/jcs.163683

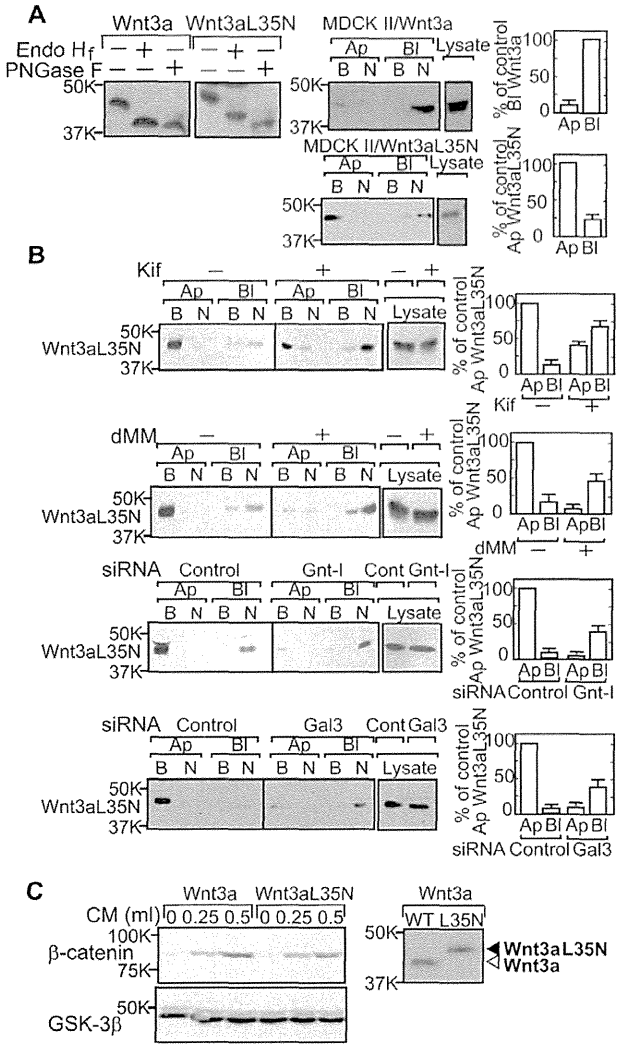

Fig. 4. Addition of the glycosylation site at the N-terminal region is sufficient to change the polarized secretion of Wnt3a. (A) Wnt3a or Wnt3aL35N in conditioned medium from MDCK II cells was precipitated using Blue–Sepharose, and the precipitates were treated with Endo H_f or PNGase F and then probed with anti-Wnt3a antibody (left panels). MDCK II cells expressing Wnt3a or Wnt3aL35N were subjected to the apical-basolateral sorting assay (right panels). The signal of Wnt3a precipitated using Neutravidin–agarose in the control basolateral (Bl) fraction or the signal of Wnt3aL35N precipitated using Blue–Sepharose in the control apical (Ap) fraction was set to 100%. B, precipitation using Blue–Sepharose; N, precipitation using Neutravidin–agarose. (B) MDCK II/Wnt3aL35N cells were treated with kif or dMM, or transfected with Gnt-I or galectin3 (Gal3) siRNA, and the cells were then subjected to the apical-basolateral sorting assay. cont, control. Results are shown as means±s.e.m. from four independent experiments. (C) L cells were stimulated with the indicated amounts of wild-type Wnt3a- or Wnt3aL35N-containing conditioned medium (CM) for 2 h, and lysates were then probed with anti-β-catenin and anti-GSK-3β antibodies (left two panels). Wild-type Wnt3a and Wnt3aL35N in conditioned medium (20 µl) are shown in the right panel. GSK-3β was used as a loading control.

Polarized localization of Wnt receptors

There are ten Frizzled (Fz) family members, which function as Wnt receptors (Kikuchi et al., 2011; Schulte and Bryja, 2007). Although the binding specificity between Wnts and Fzs is not clear, it has been shown that Fz2 mediates Wnt3a and Wnt5a signaling and that Fz7 functions as the Wnt11 receptor (Sato et al., 2010; Uysal-Onganer and Kypta, 2012). To determine the polarized localization of Fzs, MDCK II cells stably expressing FLAG–Fz2 or FLAG–Fz7 were generated (MDCK II/FLAG–Fz2 and MDCK II/FLAG–Fz7, respectively). The majority of FLAG–Fz2 was localized to the basolateral membranes, whereas FLAG–Fz7 was localized to both apical and basolateral membranes evenly (Fig. 5A–C). Knockdown of Wls did not affect the polarized localization of either Fz (Fig. 5B,C; supplementary material Fig. S1D). The polarized localization of FLAG–Fz2 was impaired in clathrin-depleted cells and cells depleted of both µ1A and µ1B (µ1A/µ1B-depleted), but not in µ4-depleted cells (Fig. 5B; supplementary material Fig. S1D,E). These results suggest that Fz2- or Fz7-loaded vesicles destined to the plasma membranes do not contain Wls, and that the basolateral localization of Fz2 requires the clathrin and AP-1 complex.

Single transmembrane receptors, including LRP6, Ror2 and Ryk, function as co-receptors of Wnt3a, Wnt5a and Wnt11, respectively (Kim et al., 2008; Nishita et al., 2010; Yamamoto et al., 2006). Although endogenous LRP6 and exogenously expressed Ror2–GFP were primarily located at the basolateral membranes of MDCK II cells (Fig. 5A,D,E), Ryk–GFP was evenly distributed in both the apical and basolateral membranes (Fig. 5A,F). Knockdown of Wls did not affect the localization of these co-receptors (Fig. 5D–F; supplementary material Fig. S1D). The basolateral membrane localization of LRP6 and Ror2–GFP was disturbed in clathrin- and µ1A/µ1B-depleted cells but not in µ4-depleted cells (Fig. 5D,E; supplementary material Fig. S1D,E).

Consistent with the polarized localization of the receptors, stimulation of polarized MDCK II/FLAG–Fz2 cells with recombinant Wnt5a at the basolateral side activated Rac1 more efficiently than that at the apical side (Fig. 5G). Recombinant Wnt3a induced LRP6 phosphorylation and the mobility shift of Dvl2 at the basolateral side more efficiently than the apical side (Fig. 5G).

Basolateral secretion of Wnt5a is required for apical lumen formation of MDCK cysts

The role of Wnt5a basolateral secretion in epithelial cells was examined by inhibiting endogenous Wnt5a synthesis and secretion in MDCK I cells. When MDCK I cells were cultured in 3D Matrigel, a nascent lumen was observed at day 4. Each cell in the cyst had a free, lateral and basal surface by acquiring polarity, and the cyst increased the lumen diameter at days 6–7, and cystogenesis was complete at days 8–9 (Fig. 6A).

Treatment of MDCK I cells with a Wnt secretion inhibitor IWP2 (Chen et al., 2009), caused a delay in lumen formation, so that a period of 10–11 days was required for formation of the lumen consisting of monolayer cells (Fig. 6A). At day 7, some cells were still observed in the luminal space of cysts treated with IWP2, and they did not make contact with the extracellular matrix (ECM) (Fig. 6A,B). Approximately 70% of cysts consisting of control MDCK I cells showed a dilated lumen, which was lined by a polarized monolayer cells, and of which the diameter was >50% that of the cyst (Fig. 6B). By contrast, treatment with IWP2 caused the number of cysts with dilated lumens to decrease, whereas the number of cysts with narrow lumens, which had multilayered cells and a diameter <50% that of the cyst, increased (Fig. 6B). Similar phenotypes were observed in Wnt5a-depleted cells (Fig. 6C; supplementary material Fig. S3A); however, knockdown of Wnt4 or Wnt7a did not affect apical lumen formation (supplementary material Fig. S3B). As well as

Journal of Cell Science (2015) 128, 1051–1063 doi:10.1242/jcs.163683

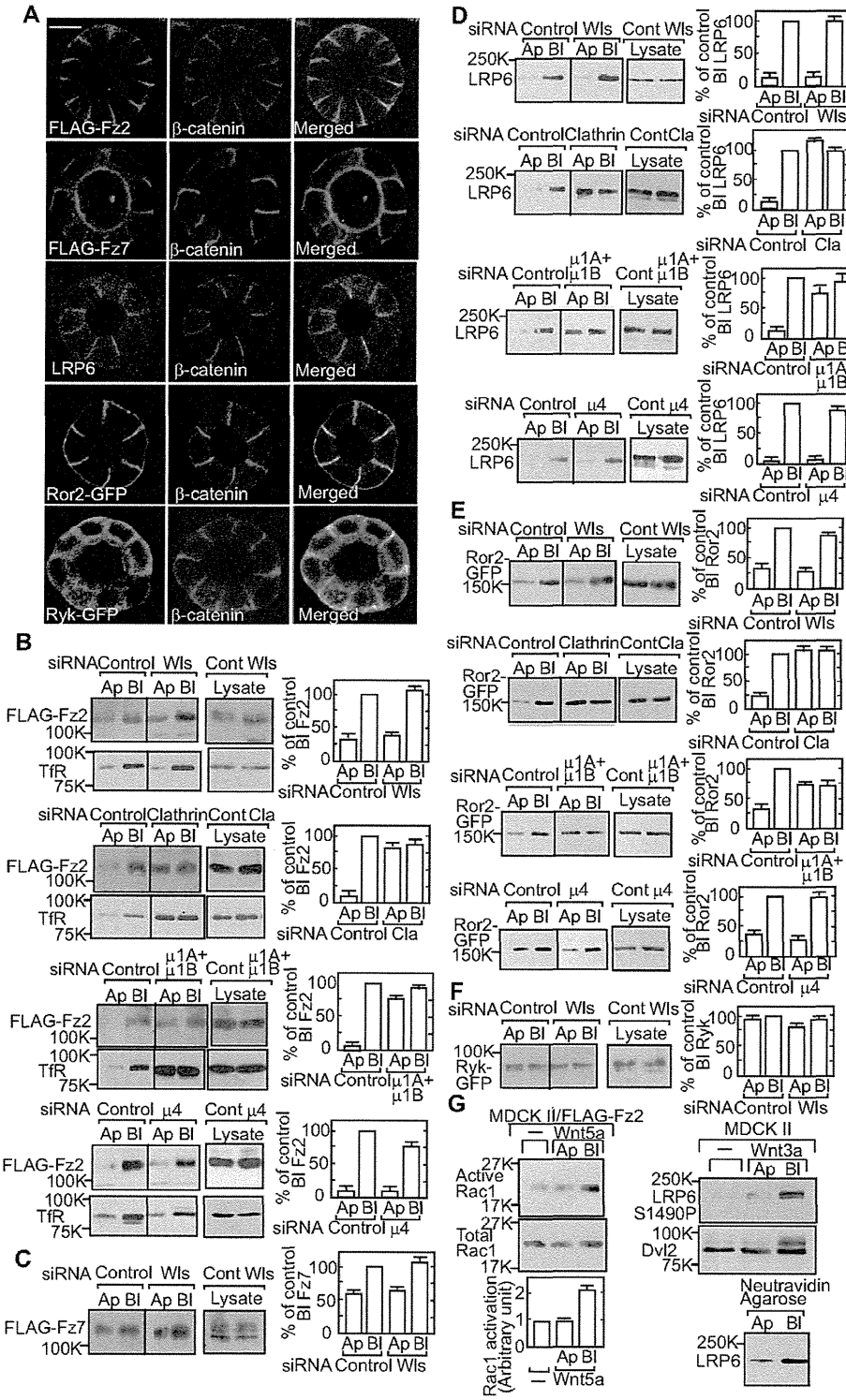

Fig. 5. The polarized localization of Wnt receptors. (A) MDCK II, MDCK II/FLAG–Fz2, MDCK II/FLAG–Fz7, MDCK II/Ror2–GFP or MDCK II/Ryk–GFP cells were cultured in 3D Matrigel, and the cysts were stained with the indicated antibodies. Scale bar: 10 μm. (B–F) MDCK II/FLAG–Fz2 (B), MDCK II/FLAG–Fz7 (C), MDCK II (D), MDCK II/Ror2–GFP (E) or MDCK II/Ryk–GFP (F) cells were transfected with siRNA for Wntless (Wls), clathrin (Cla), μ1A and μ1B, or μ4, and the cells were then subjected to the apical-basolateral sorting assay. The signal of the receptors was precipitated using Neutravidin–agarose from the control basolateral (Bl) fraction, which was set to 100%. Ap, apical; cont, control. (G) MDCK II/FLAG–Fz2 cells were stimulated with Wnt5a (50 ng/ml) (left panel) or MDCK II cells were stimulated with Wnt3a (100 ng/ml) (right panel) from the apical or basolateral sides, and lysates were then subjected to the Rac activation assay or the phosphorylation assay of LRP6 and Dvl2. Results are shown as means±s.e.m. from four independent experiments.

in MDCK II cells, apical secretion of Wnt5aL68N was observed in polarized MDCK I/Wnt5aL68N cells, and basolateral membrane localization of Ror2–GFP was observed in MDCK I/Ror2–GFP cells (supplementary material Fig. S3C). The phenotypes induced by Wnt5a siRNA were rescued by expression of wild-type Wnt5a, but not by Wnt5aL68N

Journal of Cell Science (2015) 128, 1051–1063 doi:10.1242/jcs.163683

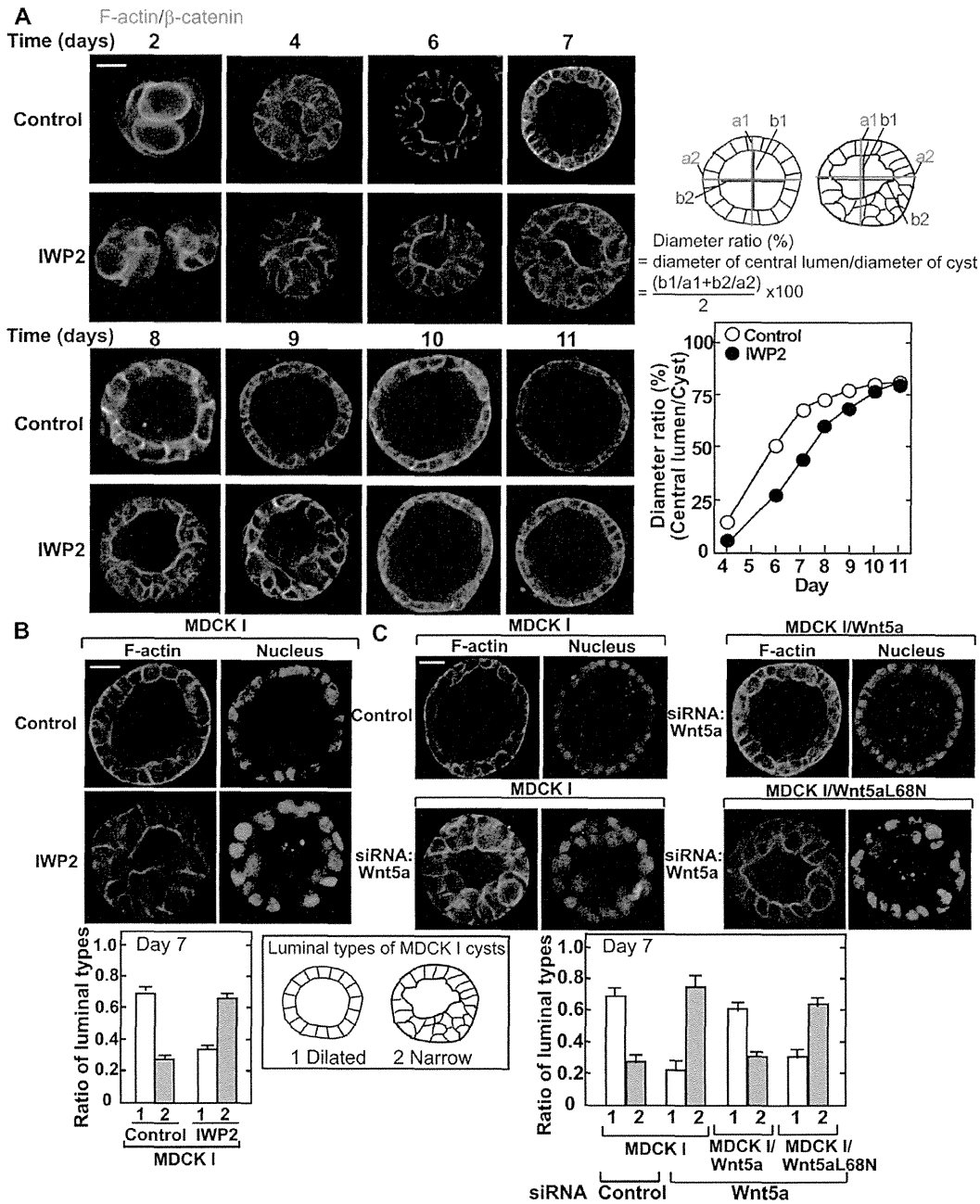

Fig. 6. Basolateral secretion of Wnt5a is required for the apical lumen formation of MDCK cyst. (A) MDCK I cells cultured in 3D Matrigel were treated with or without 5 μM IWP2 for the indicated days, and the cysts were then stained with anti-β-catenin antibody and Alexa-Fluor-488-conjugated phalloidin to visualize F-actin. The diameter ratio between the apical lumen and the whole cyst was calculated using the following formula: diameter ratio (%)=diameter of central lumen (blue line)/diameter of the cyst (red line)×100. The mean of the two diameter ratios in the cysts at the indicated days were plotted (right panel). (B) MDCK I cells cultured in 3D Matrigel were treated with or without 5 μM IWP2 for 7 days, and the cysts were then stained with Alexa-Fluor-488-conjugated phalloidin (green) and DRAQ5 (blue) to visualize the nucleus. Schematic images of MDCK I cyst with a dilated lumen (1) or narrow lumen (2) are shown. The cysts at day 7 were classified by their luminal types, and the number of cysts of each type was counted. Results are expressed as the ratio of luminal types, and are shown as the means±s.e.m. from four independent experiments. (C) MDCK I, MDCK I/Wnt5a, or MDCK I/Wnt5aL68N cells were transfected with control or Wnt5a siRNA, and the cysts were then stained with phalloidin and DRAQ5. The cysts at day 7 were classified by their luminal types. Scale bars: 20 μm.

(Fig. 6C; supplementary material Fig. S3A). These results indicate that Wnt5a signaling from the basolateral side is required for efficient apical lumen formation in MDCK I cells.

Apoptosis is required for apical lumen formation in Wnt5a-depleted cells

Treatment of MDCK I cells with IWP2 or depletion of Wnt5a suppressed the phosphorylation of FAK and paxillin at days 5–7

Journal of Cell Science (2015) 128, 1051–1063 doi:10.1242/jcs.163683

in 3D Matrigel culture (Fig. 7A), suggesting a reduction in cell-to-substrate adhesion. These manipulations also reduced Rac activity (Fig. 7B). Decreases in FAK activity, paxillin phosphorylation and Rac activity due to Wnt5a depletion were rescued by expression of wild-type Wnt5a, but not by Wnt5aL68N (Fig. 7A,B). When MDCK I cells were treated with NSC23766 (a Rac GEF inhibitor), some cells were observed in the luminal region at days 5–9, resulting in a delay of lumen formation, similar to the treatment with IWP2 and Wnt5a siRNA (Fig. 7C).

Some lumen formation models, including hollowing and cavitation, which require directional vesicle trafficking and luminal cell death, respectively, have been proposed (Datta et al., 2011). In the control cysts, very few luminal cells underwent apoptosis, whereas cysts in which Wnt5a signaling was suppressed had apoptotic cells, as determined by staining with the apoptotic marker, cleaved caspase-3 (Fig. 7C,D). Control MDCK I cysts formed a clear apical lumen with a few cells, even in the presence of the general caspase inhibitor QVD-Oph, but Wnt5a-depleted or IWP2-treated MDCK I cysts showed a decreased formation of apical lumen surrounded by monolayer cells at day 11 in the presence of QVD-Oph (Fig. 7E). Thus, apoptosis might be required for apical lumen formation in Wnt5a signaling-deficient cells. Taken together with the report that knockdown of integrins impairs apical lumen formation (Myllymäki et al., 2011), these results suggest that Wnt5a signaling promotes lumen formation by the enhancement of cell-to-substrate adhesion through integrins.

DISCUSSION

Polarized secretion of Wnt5a

It is believed that the trafficking of some apically sorted proteins is dependent on glycosylphosphatidylinositol-anchor-interacting signals or glycan-mediated signals, whereas basolaterally sorted proteins are delivered by the interaction of cytoplasmic trafficking signals with sorting machineries such as clathrin and APs (Boehm and Bonifacino, 2001; Deborde et al., 2008; Fölsch, 2005; Vagin et al., 2009). In this study, we determined the profiles of glycans attached to Wnt5a by ESI-MS/MS. N114 and N326 of Wnt5a were modified with high-mannose-type glycans. Both Asn residues are conserved in most Wnts, and modification with high-mannose-type glycan was also observed at the conserved Asn residues of Wnt3a and Wnt11 (Yamamoto et al., 2013). By removing both high-mannose-type glycans, the secretion of Wnt3a, Wnt5a and Wnt11 was impaired, suggesting that these glycans are necessary for maintaining the overall folded structure. Wnt5a was also modified with hybrid-type glycan at N312, although it was not essential for secretion because the Wnt5aN312Q mutant displayed secretion comparable to that of wild-type Wnt5a. The glycosylation site is unique in Wnt5a and Wnt5b, but the role of glycosylation at this site remains unknown.

Wnt5a and Wnt3a were secreted apically following the addition of the glycosylation site at their N-terminal region (Wnt5aL68N and Wnt3aL35N). The complex-type glycan was attached to the glycosylation site, and their apical secretion depended on galectin-3, similar to that of Wnt11. Therefore, Wnts that are modified with the complex-type glycan at the N-terminal region might be secreted apically by galectin-3. It is noteworthy that a single amino acid substitution of Wnt is able to change its trafficking route without causing it to lose activity.

The Wnt5a basolateral secretion is likely to be mediated by the same mechanism as that of Wnt3a (Yamamoto et al., 2013), because its sorting requires clathrin and AP-1, which are common machineries for the basolateral sorting of membrane proteins (Boehm and Bonifacino, 2001). Given that Wls is also trafficked to the basolateral membrane, and is recognized by palmitoleic-acid-modified Wnts (Port and Basler, 2010; Yamamoto et al., 2013), Wls should localize to Wnt5a- and Wnt3a-loaded vesicles.

Polarized trafficking of Wnt receptors

Drosophila Fz1 (dFz1) and dFz2 act as receptors for wingless, a *Drosophila* Wnt homolog. Both receptors mediate the β-catenin-dependent pathway, and dFz1 also functions in the β-catenin-independent pathway, especially the planar cell polarity (PCP) pathway (Strutt, 2003). dFz1 is concentrated at apical junctions in the wing imaginal disc, whereas dFz2 is distributed throughout the apical and basolateral membranes (Wu et al., 2004). The C-terminal cytoplasmic amino acid sequence of dFz2 prevents it from accumulating at the apical junctions, and the apical localization of dFz1 is necessary for the activation of the PCP pathway. These results suggest that it is the localization of the receptors that determines pathway specificity.

Our study showed that Fz2 mainly localized to the basolateral membranes in MDCK II cells, whereas Fz7 was relatively evenly distributed throughout the apical and basolateral membranes. Fz2 acts as a common receptor for Wnt3a and Wnt5a (Sato et al., 2010), and Fz7 functions as a receptor for Wnt11 (Kim et al., 2008; Yamanaka and Nishida, 2007). LRP6 and Ror2, which are receptors for Wnt3a and Wnt5a, respectively (Nishita et al., 2010; Yamamoto et al., 2006), were also trafficked to the basolateral membranes using clathrin and AP-1. Ryk, which mediates Wnt11 signaling (Kim et al., 2008), was localized to both the apical and basolateral membranes. Because Wnt3a and Wnt5a are secreted basolaterally and Wnt11 is secreted apically, the localization of their receptors in polarized MDCK II cells is understandable. The signaling pathways of Wnt3a and Wnt5a were strongly activated when both Wnts stimulated the basolateral side, indicating that localization of their receptors is functionally coupled to the polarized secretion of Wnts. Thus, it is likely that the appropriate Wnt receptors are sorted to the same polarized fractions as the corresponding Wnts, thereby leading to efficient activation of their signals.

Our results are consistent with the findings that Ror2 is localized to the basal sides of the embryonic midgut epithelium (Yamada et al., 2010), and that LRP6 is present in the basolateral region of *Xenopus* outer ectodermal cells (Huang and Niehrs, 2014). Wls is essential for the trafficking of Wnts (Port and Basler, 2010), but it is not required for the apical and basolateral sorting of Wnt receptors. Therefore, Wnt-loaded vesicles could be distinct from vesicles containing their receptors, which probably prevents intracellular activation of Wnt signaling by the co-existence of ligands and receptors in the same vesicles. An alternative possibility might be that Wnts and Wnt receptors are loaded in the same vesicle containing Wls and that there is a mechanism to inhibit their binding.

Regulation of apical lumen formation by basolateral secretion of Wnt5a

We have shown previously that Wnt5a is involved in the single-cell polarization of rat intestinal epithelial IEC6 cells through Rac1 activation (Gon et al., 2013), and that Wnt5a promotes cell-to-substrate adhesion in cancer cells (Matsumoto et al., 2010). Other studies have demonstrated that Rac1 activation at the basolateral side is required for the polarization of MDCK cysts (Yagi et al., 2012), and that knockdown of integrins impairs apical lumen formation in MDCK cells (Myllymäki et al., 2011).

Journal of Cell Science (2015) 128, 1051–1063 doi:10.1242/jcs.163683

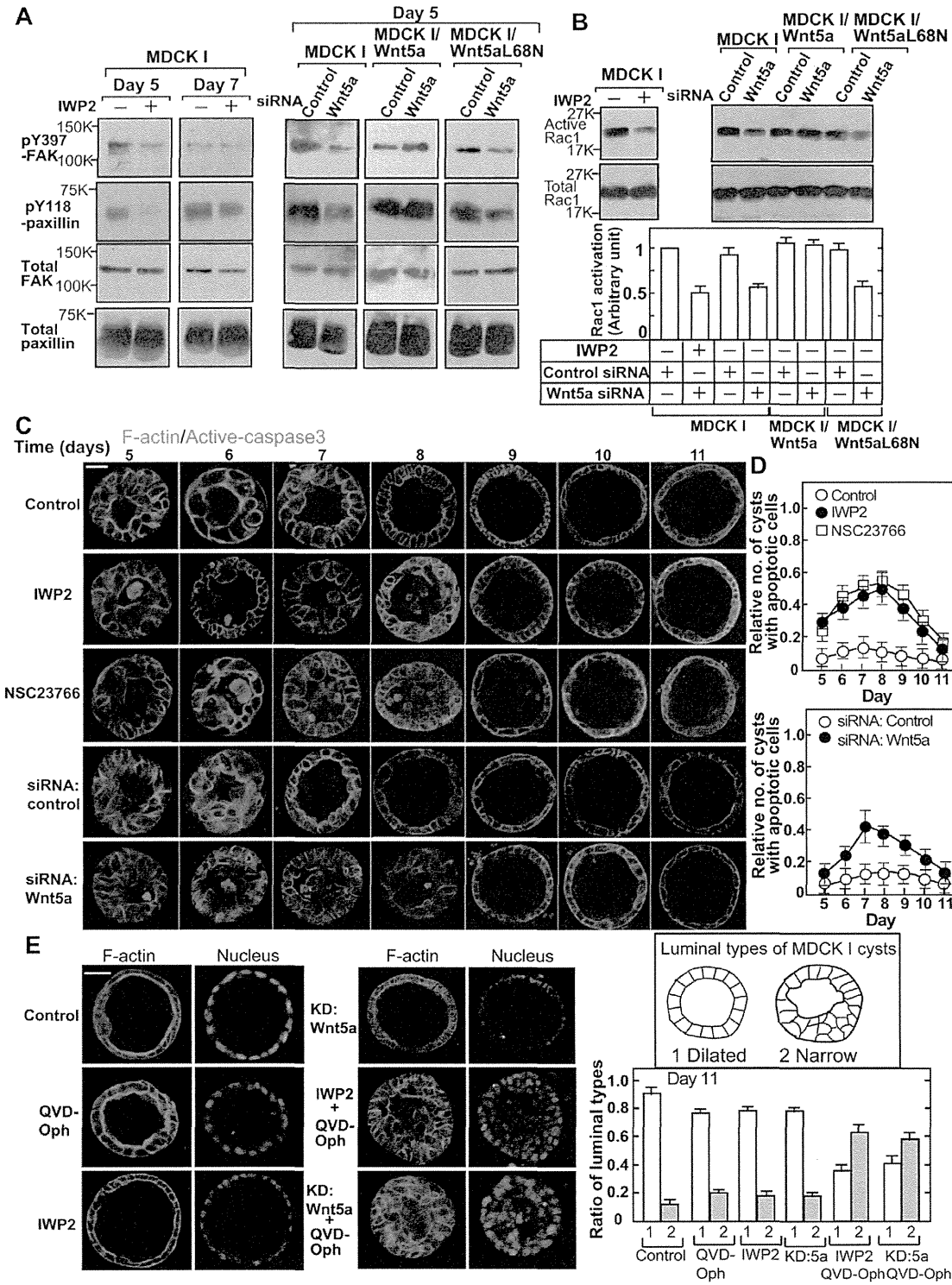

Fig. 7. See next page for legend.

However, it is not clear how these cellular events are linked to form apical lumen in polarized epithelial cells.

Lumen formation relies on the coordination of cell-to-substrate recognition, apical and basal polarization, and lumen expansion (Datta et al., 2011). Thus, cell adhesion to ECM is the first event for luminogenesis. Wnt5a secretion enhances cell-to-substrate adhesion in 3D culture. During MDCK cystogenesis in type I collagen gel, Rac1 activities are necessary for orientation of apical polarization through assembly of the basolateral laminin (O'Brien et al., 2001). Because our 3D culture was performed

Fig. 7. Apoptosis is required for the apical lumen formation in Wnt5a-depleted cells. (A) MDCK I, MDCK I/Wnt5a, or MDCK I/Wnt5aL68N cells were cultured in Matrigel in the presence or absence of IWP2 (left two panels) or transfected with control or Wnt5a siRNA (right three panels) for 5 or 7 days, and cell lysates at day 5 or 7 were then probed with anti-pY397-FAK and anti-pY118-paxillin antibodies. FAK and paxillin were used as loading controls. (B) MDCK I, MDCK I/Wnt5a or MDCK I/Wnt5aL68N cells were cultured in the presence or absence of IWP2, or were transfected with control or Wnt5a siRNA for 7 days, and cell lysates at day 7 were then subjected to the Rac activation assay. (C) MDCK I cells in 3D culture were treated with 5 μM IWP2 or NSC23766, or transfected with control or Wnt5a siRNA for the indicated days, and the cysts were then stained with anti-active caspase3 antibody (red) and Alexa-Fluor-488-conjugated phalloidin (green). (D) Quantification of cysts having apoptotic cells in the lumen from 5–11 days in panel C. Results are shown as the means±s.e.m. from three independent experiments. (E) MDCK I cells treated with IWP2 or transfected with Wnt5a siRNA were incubated with 10 μM QVD-Oph for 11 days, and the cysts were stained with phalloidin and DRAQ5. The cysts at day 11 were classified by their luminal types, and the number of cysts of each type was counted. Results are shown as the means±s.e.m. from four independent experiments. Scale bars, 20 μm.

using Matrigel-containing laminin, Wnt5a-dependent Rac activation in MDCK I cells would not be required for laminin assembly, but would be involved in apical lumen formation. It has been reported that when apical and basolateral polarity is acquired efficiently or when cell polarity is coordinated with cell proliferation in MDCK cells, membrane separation without apoptosis in the center of the cord is sufficient for lumen formation (Martín-Belmonte et al., 2008). However, when apical and basolateral polarization is achieved slowly, apoptosis is required for clearance of the lumen. The results in this study showed that manipulations that inhibit Wnt5a signaling cause a delay in lumen formation. Apoptosis occurred to eliminate cells in the luminal space in these cysts. The phenotypes induced by Wnt5a knockdown were rescued by wild-type Wnt5a, but not by apically secreted Wnt5a. Taken together, these data suggest that polarized secretion of Wnt5a stimulates adhesion-dependent Rac activation and acquisition of apical and basolateral polarization, thereby enhancing lumen formation without apoptosis.

Wnt5a is expressed in the epithelium of the urogenital sinus, hindgut and cloacal membrane during development, and in adult uterine luminal epithelial cells (Daikoku et al., 2011; Li et al., 2011). MDCK I and IEC6 cells are good cell lines for analyzing endogenous Wnt5a roles in polarized epithelial cells. In these cells, the Wnt5a–Fz2–Ror2 axis might be involved in the establishment of apical and basolateral polarization in an autocrine manner. However, because mesenchymal cells are the primary source of Wnt5a secretion, epithelial cells that express Wnt5a receptors at the basolateral membranes might receive Wnt5a secreted from mesenchymal cells. For example, Wnt5a and Ror2 are expressed in the mesenchyme and epithelial basal region of embryonic midgut; aberrant epithelial cell clumps, which suggest polarity loss and random orientation of cells, are observed in Ror2-knockout embryonic gut (Yamada et al., 2010). In summary, Wnt5a and its receptors are trafficked to the basolateral side of polarized epithelial cells by different mechanisms, and the basolateral secretion of Wnt5a is necessary for apical lumen formation without apoptosis.

MATERIALS AND METHODS

Materials and chemicals

pPGK-neo/mouse Wnt5a, pRK5/rat Fz2 and pRK5/mouse Fz7 were provided by Dr Shinji Takada (National Institutes of Natural Sciences, Okazaki, Japan). pEGFP-N3/mouse Ror2, p3xFLAG-CMV/rat Ryk and pCB6/μ1B-HA were from Drs Yasuhiro Minami (Kobe University, Kobe, Japan), Keiko Ohsawa and Shinichi Kohsaka (National Center of Neurology and Psychiatry, Tokyo, Japan) and Heike Fölsch (Northwestern University, Chicago, IL), respectively. Wnt5a was purified to homogeneity (Kurayoshi et al., 2007). Anti-Wnt5a (for immunostaining) was generated as described previously (Sato et al., 2010). Other primary antibodies used in this study are listed in supplementary material Table S3. FLAG–Fz7, Ryk–GFP and μ1B–HA cDNAs were cloned into pCSII-CMV-MCS-IRES2-Bsd to construct lentiviral vectors (Takara Bio Inc., Shiga, Japan). pLvSIN/FLAG–Fz2 was constructed as described previously (Fumoto et al., 2012). Standard recombinant DNA techniques were used to construct pPGK-neo/Wnt5a mutants. RNA duplexes and forward and reverse primers for quantitative real-time PCR used in this study are shown in supplementary material Tables S4, S5. PNGase F and Endo H_f were from Roche Diagnostics GmbH (Mannheim, Germany) and New England Biolabs (Beverly, MA), respectively. Other materials were obtained from commercial sources.

Cell culture and transfection

MDCK I and II, L, X293T and NIH3T3 cells were maintained in Dulbecco's modified Eagle's medium (DMEM) supplemented with 10% fetal bovine serum (FBS). HEK293T cells were maintained in DMEM/Ham's F12 supplemented with 10% FBS. L or MDCK cells stably expressing wild-type Wnt5a, wild-type Wnt3a or their mutants were generated by selection with G418. To transiently express Ror2–GFP or Wnt5a, MDCK II cells were transfected with plasmids using Fugene HD (Promega, Madison, WI). MDCK II cells stably expressing FLAG–Fz7 or Ryk–GFP were generated by infection with lentiviruses. Then, the cells were selected and maintained in the same medium containing 2.5 μg/ml blasticidin S. Three independent clones of each stable cell line were used for experiments to avoid clonal variation, and similar results were obtained.

Immunofluorescence microscopy

To visualize the intracellular localization of Wnts or their receptors in 3D Matrigel, the cells were fixed for 30 min in PBS containing 4% (w/v) paraformaldehyde (PFA) and then permeabilized with PBS containing 0.5% (w/v) Triton X-100 and 4% (w/v) BSA for 30 min. For staining of endogenous LRP6 or Ror2–GFP, cells were fixed with 100% methanol at −20°C for 30 min, washed with PBS three times and blocked for 30 min in 1% BSA in PBS containing 0.2% Triton X-100. To observe extracellularly secreted Wnt5a, MDCK II cells transiently expressing Wnt5a in 3D Matrigel were incubated with medium containing anti-Wnt5a antibody (1:100 dilution) for 1 h in a heated chamber (37°C, 5% CO_2), washed with PBS three times and fixed for 30 min in PBS containing 4% PFA. Then, the cells were incubated with goat Alexa-Fluor-488-conjugated anti-rabbit-IgG without permeabilization. Then, the cells were stained with anti-Wnt5a, anti-LRP6, anti-GFP, anti-FLAG, anti-β-catenin or anti-active caspase 3 antibodies for 2 h. Cells were washed with PBS three times and incubated with goat Alexa-Fluor-488- or Alexa-Fluor-546-conjugated anti-mouse- or anti-rabbit-IgG, and Alexa-Fluor-488-, Alexa-Fluor-546- or Alexa-Fluor-633-conjugated phalloidin (Life Technologies, Carlsbad, CA) to visualize F-actin for 2 h. If necessary, nuclei were counterstained with a 1:1000 dilution of DRAQ5 (BioStatus Ltd, Shepshed, UK). The cells were then washed three times, mounted on slides and viewed using a confocal microscope (LSM510, Carl Zeiss, Jana, Germany).

Preparation of glycopeptides and lipopeptides of Wnt5a

Glycopeptides and lipopeptides of Wnt5a were prepared as described previously (Yamamoto et al., 2013). Briefly, after Wnt5a (1 μg) was separated by SDS-PAGE, the protein bands were excised from the gel and were incubated with 50 nM trypsin (Promega) in 20 mM ammonium bicarbonate and 10% acetonitrile at 37°C for 16 h. The tryptic peptides were extracted with 100 μl of 0.1% trifluoroacetic acid in 10% acetonitrile/H_2O for glycosylation analysis, followed by 100 μl of 0.1% trifluoroacetic acid in 60% acetonitrile/H_2O for lipidation analysis.

Nano-flow liquid chromatography/matrix-assisted laser desorption/ionization mass spectrometry

Tryptic digests of Wnt5a were injected into an Ultimate nano-LC system (Dionex, Idstein, Germany), and overall peptide identification was then carried out using a MALDI-TOF/TOF (4700 proteomics analyzer, Applied Biosystems, Framingham, MA) as described previously (Awada et al., 2010).

Nano-flow liquid chromatography/electrospray ionization mass spectrometry

To examine the glycan chains and relative abundance of each glycoform at each glycosylation site, the above tryptic digests were applied to a PicoFrit C18 column (0.075 mm×100 mm, Inertsil 3-μm particle size, NewObjective), and the eluates were then continuously analyzed by a linear ion-trap/time-of-flight mass spectrometer equipped with a nano-flow electrospray ion source (Hitachi NanoFrontier LD, Hitachi High-Technology, Tokyo, Japan) as described previously (Kimura et al., 2013).

Apical-basolateral sorting assay

Polarized sorting of Wnt5a and Wnt receptors was examined as described previously (Yamamoto et al., 2013). MDCK I or II cells (2×10^5 cells) expressing Wnt5a, Wnt3a, their mutants or Wnt receptors were seeded on transwell polycarbonate filters (Corning Costar Quality Biological, Gaithersburg, MD) for 7 days (MDCK I cells) or 3 days (MDCK II cells). Media from the apical and basolateral sites were precipitated with Blue–Sepharose to detect Wnts secreted into the culture medium (indicated as 'B' in figures). To detect membrane cell-surface-associated Wnts or their receptors, the apical or basolateral surface membranes of the cells were selectively incubated with 0.5 mg/ml sulfo-NHS-LC-biotin (Pierce Biotechnology, Rockford, IL) for 30 min at 4°C (Sakane et al., 2012; Yamamoto et al., 2013). Biotinylated proteins were precipitated using Neutravidin–Agarose (Pierce Biotechnology), and the precipitates were probed using each antibody (indicated as 'N' in figures).

3D culture of MDCK cells

MDCK cells were suspended in Matrigel (BD Biosciences, San Jose, CA) at a density of 1×10^4 cells/ml, and 80 μl of the cell suspension was mounted on a round coverslip as described previously (Yamamoto et al., 2013). After incubation at 37°C for 30 min to solidify the gel, the cells on the coverslip were transferred to a 24-well culture plate and incubated in 1 ml of DMEM containing 10% FBS for 7 days (MDCK I cells) or 3 days (MDCK II cells). Under the conditions, MDCK cells formed cysts. For treatment with inhibitors, 5 μM IWP2, 5 μM NSC23766 or 10 μM QVD-Oph were added when plating in Matrigel, and medium was changed every 2 days.

Knockdown of mRNA in MDCK cells by siRNA

To transfect siRNA into MDCK cells expressing Wnt5a or its receptors, trypsinized MDCK cells were suspended in Opti-MEM (Life Technologies) at 10^6 cells per 100 μl, siRNA was added (160 pmol), and cells were electroporated using NEPA21 (NEPAGENE, Tokyo, Japan) with five square pulses of 20 V of 50-ms duration (Yamamoto et al., 2013). After cells were consecutively transfected twice at 2-day intervals, knockdown cells (2×10^5 cells) were seeded on a Transwell polycarbonate filter for an additional 3 days.

Statistical analysis

Experiments were performed at least four times, and the results are expressed as means±s.e.m. Statistical analysis was performed using StatView software (SAS Institute, Inc., Cary, NC). Differences between the data were tested for statistical significance using Student's *t*-test. Two-tailed *P*-values less than 0.05 were considered statistically significant.

Additional methods

Methods for quantitative real-time PCR were as described previously (Sato et al., 2010; Yamamoto et al., 2013). Preparation of conditioned medium, the extracellular matrix (ECM) fraction and lysates from Wnt-producing cells were performed as described previously (Komekado et al., 2007; Kurayoshi et al., 2007).

Acknowledgements

We thank Drs S. Takada, Y. Minami, K. Ohsawa, S. Kohsaka, and H. Fölsch for donating plasmids.

Competing interests

The authors declare no competing or financial interests.

Author contributions

H.Y. designed experiments, carried out purification of Wnt proteins, performed the apical-basolateral sorting assay and immunofluorescence analyses, and wrote the manuscript. S.M. performed immunofluorescence analyses. T.K. carried out the apical-basolateral sorting assay. T.S. performed the fractionation assay. C.A. and T.T. analyzed the glycosylation and lipidation profiles of Wnt5a by mass spectrometry and provided advice. A.K. designed the experiments and wrote the manuscript.

Funding

This work was supported by Grants-in-Aid for Scientific Research (2009–2011) [grant number 21249017], for Scientific Research on Priority Areas (2011–2013) [grant number 23112004] to A.K., and for Scientific Research (2011–2013) [grant number 23590333] and (2014–2016) [grant number 26460365] to H.Y. from the Ministry of Education, Science and Culture of Japan; and by a research grant in the natural sciences from the Mitsubishi Foundation (2013–2014) [grant number 25117]; and by the NOVARTIS Foundation (Japan) for the Promotion of Science (2013) to A.K. T.S. is supported by the Osaka University Faculty of Medicine Medical Doctor Scientist Training Program.

Supplementary material

Supplementary material available online at
http://jcs.biologists.org/lookup/suppl/doi:10.1242/jcs.163683/-/DC1

References

Awada, C., Sato, T. and Takao, T. (2010). Affinity-trap polyacrylamide gel electrophoresis: a novel method of capturing specific proteins by electro-transfer. *Anal. Chem.* **82**, 755-761.

Boehm, M. and Bonifacino, J. S. (2001). Adaptins: the final recount. *Mol. Biol. Cell* **12**, 2907-2920.

Bryant, D. M. and Mostov, K. E. (2008). From cells to organs: building polarized tissue. *Nat. Rev. Mol. Cell Biol.* **9**, 887-901.

Chen, B., Dodge, M. E., Tang, W., Lu, J., Ma, Z., Fan, C. W., Wei, S., Hao, W., Kilgore, J., Williams, N. S. et al. (2009). Small molecule-mediated disruption of Wnt-dependent signaling in tissue regeneration and cancer. *Nat. Chem. Biol.* **5**, 100-107.

Daikoku, T., Cha, J., Sun, X., Tranguch, S., Xie, H., Fujita, T., Hirota, Y., Lydon, J., DeMayo, F., Maxson, R. et al. (2011). Conditional deletion of Msx homeobox genes in the uterus inhibits blastocyst implantation by altering uterine receptivity. *Dev. Cell* **21**, 1014-1025.

Datta, A., Bryant, D. M. and Mostov, K. E. (2011). Molecular regulation of lumen morphogenesis. *Curr. Biol.* **21**, R126-R136.

Deborde, S., Perret, E., Gravotta, D., Deora, A., Salvarezza, S., Schreiner, R. and Rodriguez-Boulan, E. (2008). Clathrin is a key regulator of basolateral polarity. *Nature* **452**, 719-723.

Dukes, J. D., Whitley, P. and Chalmers, A. D. (2011). The MDCK variety pack: choosing the right strain. *BMC Cell Biol.* **12**, 43.

Elbein, A. D., Tropea, J. E., Mitchell, M. and Kaushal, G. P. (1990). Kifunensine, a potent inhibitor of the glycoprotein processing mannosidase I. *J. Biol. Chem.* **265**, 15599-15605.

Fölsch, H. (2005). The building blocks for basolateral vesicles in polarized epithelial cells. *Trends Cell Biol.* **15**, 222-228.

Fuhrmann, U., Bause, E., Legler, G. and Ploegh, H. (1984). Novel mannosidase inhibitor blocking conversion of high mannose to complex oligosaccharides. *Nature* **307**, 755-758.

Fumoto, K., Kikuchi, K., Gon, H. and Kikuchi, A. (2012). Wnt5a signaling controls cytokinesis by correctly positioning ESCRT-III at the midbody. *J. Cell Sci.* **125**, 4822-4832.

Furuse, M., Furuse, K., Sasaki, H. and Tsukita, S. (2001). Conversion of zonulae occludentes from tight to leaky strand type by introducing claudin-2 into Madin-Darby canine kidney I cells. *J. Cell Biol.* **153**, 263-272.

Gon, H., Fumoto, K., Ku, Y., Matsumoto, S. and Kikuchi, A. (2013). Wnt5a signaling promotes apical and basolateral polarization of single epithelial cells. *Mol. Biol. Cell* **24**, 3764-3774.

Gottardi, C. J., Dunbar, L. A. and Caplan, M. J. (1995). Biotinylation and assessment of membrane polarity: caveats and methodological concerns. *Am. J. Physiol.* **268**, F285-F295.

Gravotta, D., Carvajal-Gonzalez, J. M., Mattera, R., Deborde, S., Banfelder, J. R., Bonifacino, J. S. and Rodriguez-Boulan, E. (2012). The clathrin adaptor AP-1A mediates basolateral polarity. *Dev. Cell* **22**, 811-823.

Harterink, M. and Korswagen, H. C. (2012). Dissecting the Wnt secretion pathway: key questions on the modification and intracellular trafficking of Wnt proteins. *Acta Physiol. (Oxf.)* **204**, 8-16.